

# (Mis)allocation of Renewable Energy Sources\*

Stefan Lamp<sup>†</sup>      Mario Samano<sup>‡</sup>

April 28, 2022

## Abstract

Policies to incentivize the adoption of renewable energy sources usually offer little flexibility to adapt to heterogeneous benefits across locations. We evaluate the geographical misallocation of solar photovoltaic installations and their relation with the uniform nature of subsidies. We estimate the dispersion of marginal benefits from solar production in Germany and compute the social and private benefits from optimal reallocations of residential solar installations keeping total capacity fixed. Our findings suggest that the value of solar would increase by 5.2% relative to the current allocation using conservative values for the rates of solar installations. Reallocating all solar capacity and taking into account transmission would yield gains that range from about 16 to 30%. A benefit-cost analysis shows that additional transmission can be beneficial if there is sufficient solar capacity reallocated across regions. This puts in perspective the social costs of nation-wide policies that do not offer heterogeneous incentives.

JEL codes: H23, Q42, Q48, Q51

Keywords: Solar energy, electricity markets, feed-in-tariffs, ancillary services, misallocation.

---

\*We thank Stefan Ambec, Bob Cairns, Estelle Cantillon, Natalia Fabra, Karlo Hainsch, Pär Holmberg, Gordon Leslie, Mar Reguant, Francois Salanie, Steve Salant, Thomas Tangeras, and seminar participants at the TSE-UC3M Energy Workshop, Mannheim Energy Conference, University of Quebec at Montreal, Toulouse School of Economics, IAEE, CEA 2019, and EAERE 2019 for their comments. We are also indebted to the Editor and the anonymous referees for their insightful feedback. This project has received funding from the European Research Council (ERC) under the European Union's Horizon 2020 research and innovation program (grant agreement No 772331). Mario Samano acknowledges financial support from the SSHRC and the FQRSC.

<sup>†</sup>Universidad Carlos III Madrid. Email: [slamp@eco.uc3m.es](mailto:slamp@eco.uc3m.es)

<sup>‡</sup>HEC Montreal. Email: [mario.samano@hec.ca](mailto:mario.samano@hec.ca)

# 1 Introduction

Climate change mitigation policies largely rely on the adoption of renewable energy sources (RES). Yet, to many policy-makers, the decision to introduce specific types of RES such as solar photovoltaic (PV) in electricity markets hinges on the size of its economic impacts. Electricity from solar PV plants is still more costly than from conventional technologies in some regions, it is not perfectly correlated with demand, its intermittency is problematic, it is non-dispatchable, and the storage costs for electricity are relatively high (Baker et al. [2013]). Feed-in-Tariffs (FiTs), a widely used policy to incentivize the deployment of solar and other RES, guarantee a preferential rate paid to solar producers of electricity. They are regulated by the government, specify long-term contracts of about 15 to 20 years, and they have been implemented in a number of jurisdictions including Australia, California, Germany, Ontario, and Spain. Usually the incentives differ by RES technology, i.e. solar versus wind, but do not account for the relative productivity of the technology or their marginal benefits, which largely depend on the specific location of the plant.

This paper provides a framework to quantify empirically the extent of misallocation of solar PV plants, potentially driven by the lack of location-specific incentives in uniform FiT-type policies. Our contributions consist of three sets of results. First, making use of an extensive and high-frequency dataset on electricity production and demand, we measure the benefits from an additional unit of electricity output from solar due to the displacement of production from conventional sources. These benefits include the private costs of production and grid reliability as well as the social costs of the emissions displaced. These results quantify the heterogeneity in the effects from solar across different subregions from the same electricity market where a FiT policy has been implemented as a uniform incentive. Our findings underline the misalignment between the policy design and the heterogeneity of the solar productivity and their benefits.

Second, we construct a series of counterfactual scenarios in which solar capacity gets reallocated from regions with low marginal benefits into regions with higher marginal benefits to maximize its benefits while keeping the total amount of solar capacity constant within the

entire market. Then we simulate the output in each of those counterfactual scenarios and compare the total gains against those from the actual allocation. Albeit the gains being positive by construction, it is an empirical question what the magnitude of such gains is.

Third, electricity trade is an important factor in the reallocation of output from solar and therefore, we calculate the gains from an increase in transmission capacity between subregions. We compute the shadow cost of transmission and use it to back out the implied size of the transmission capacity. Then, we reallocate solar capacity assuming that the transmission capacity is expanded within a pre-estimated range and compute the gains from reallocation for different levels of capacity expansion.

Since most FiT programs have very small or no variation in the amount of the incentive on output by geographical location or by time of the day, it is an empirical question whether this corresponds to a lack of variation in the marginal benefits of solar power.<sup>1</sup> We focus our analysis on solar power in Germany, which has been the first country to implement large-scale FiTs for RES. [Fell and Linn \[2013\]](#) call the German case the *most prominent* example of this policy.<sup>2</sup> While FiTs have been an effective tool in increasing the penetration of RES, they are also expensive. In 2015 alone the total subsidy accounted for roughly 22 billion euros and financing the subsidy has led to an intense political debate about how to distribute the total cost between different consumer groups ([Gerster and Lamp \[2020\]](#)). The location of solar plants also has implications for the dispersion of benefits from new products such as electric vehicles ([Holland et al. \[2016\]](#)) and for electricity storage ([Sinn \[2017\]](#), [Zerrahn et al. \[2018\]](#)).<sup>3</sup>

---

<sup>1</sup>[Borenstein and Bushnell \[2022\]](#) document how the social marginal costs of electricity in the U.S. are in some regions above and in others below the retail price of electricity, which shows that if those prices were to be used for indexing tariffs, they would not correctly account for the potential benefits. [Fowle and Muller \[2019\]](#) show through a theory model that under perfect information and heterogeneous damages, a non-uniform tax policy over damages is welfare improving, but these results turn ambiguous when there is no perfect information.

<sup>2</sup>We abstract from other forms of incentives in Germany, particularly for wind production, known as “technology banding” where there is heterogeneity in the incentives by giving an advantage to producers in locations with lower output productivity (see [Fabra and Montero \[2022\]](#) for a theoretical analysis). By concentrating only on solar energy, we provide a conservative measure of the inefficiency of this policy. The addition of wind capacity to our analysis would at best leave our estimates unchanged, but otherwise the potential gains from reallocation would increase.

<sup>3</sup>Other studies have focused on finding a solution to the social planner’s cost-minimization problem of allocating production. One example is [Carvallo et al. \[2020\]](#), who allocate the new solar capacity proportionally

The average marginal benefit in each region can be decomposed into three main elements: displaced emissions, avoided operating costs, and avoided ancillary services. Our results show that although the heterogeneity in average marginal overall benefits across regions ranges only from 41.01 to 44.8 €/MWh, their components contain a large range of variation. The mean avoided production costs across TSOs ranges from 19.3 to 29.4 €/MWh. The largest amounts of avoided CO<sub>2</sub> emissions do not coincide with the largest savings in operating costs due to the differences in the technology portfolio mix in each TSO. The avoided ancillary costs constitute up to 2% of the overall marginal benefits on average, but with large standard deviations.

Then we calculate the social and private costs from the potential misallocation of solar PV plants. First, we focus on small-scale residential solar installations and perform a counterfactual allocation of those plants starting in regions with the highest marginal benefits. We do this in each TSO while keeping the total solar capacity in the market constant so that our results reflect solely the effects of reallocation and not of additions to the system. We define the *feasible solar penetration rate* as a constraint that the counterfactual installations of solar PV on residential buildings cannot exceed. As this rate increases, more of the existing solar capacity gets allocated to the regions with the highest benefits until all the available solar capacity is placed in one region. Our results show a 5.2% of gains in value (ancillary services, avoided production costs, and avoided emissions combined) relative to the current allocation, assuming a feasible solar penetration rate of 20%. We also consider two alternative mechanisms to reallocate the solar capacity, one that uses only the differences in solar irradiation and another that constructs a single marginal cost curve for all of Germany instead of TSO-specific curves. In general, our results are similar across those three specifications.

Second, we extend the analysis to include all solar capacity while adapting the feasible solar penetration rate definition accordingly. An important policy aspect when discussing reallocation in this case is the transmission capacity. In order to study this, we split the largest TSO stretching from North to South Germany into two parts, with different average

---

to the area of the utility and not as a function of the marginal benefits.

solar productivity, making the South region a net exporter of solar to the North region.<sup>4</sup> Then, we perform a counterfactual allocation of total installed solar capacity in Germany, taking into account the transmission constraint that allows the South region to export solar electricity to the North. We find gains from reallocation that range from approximately 16% to 30% at intermediate values of the feasible solar penetration rate, but can be considerably larger for higher levels of transmission capacity and the solar rate. Applying these figures to a benefit-cost analysis for one of the current projects under construction, we conclude that the net benefits of the project can be positive, even without accounting for other forms of RES or other interconnections when sufficient capacity is allocated in the region with the highest total benefits.<sup>5</sup>

Our work is related to the literature that quantifies the value of the marginal output from RES (Callaway et al. [2018]), the value of displaced emissions in electricity markets using the exogeneity of wind and solar output (Abrell et al. [2019a], Cullen [2013], Novan [2015]), and the costs from the fluctuations in ancillary services due to RES expansions (Tangeras and Wolak [2019]). Our reallocation counterfactuals have similarities to those in Asker et al. [2019] for oil extraction and in Sexton et al. [2021] for solar panels. However, our work differs from the latter in that we use actual solar output data instead of output from a simulation model, our definition of benefits includes health benefits through the social cost of carbon of emissions avoided, and the savings from production and ancillary services costs, which has received little to no attention in the literature.<sup>6</sup> In our analysis of misallocation and trade, we extend the applicability of the methods in Joskow and Tirole [2005] and LaRiviere and Lyu [2022], which contrast with those using natural experiments as in Davis and Hausman [2016]. Similarly to Fell et al. [2020], we also exploit the price spread across regions as evidence of congestion.<sup>7</sup>

---

<sup>4</sup>We estimate that the average transmission capacity consistent with the observed gap in marginal costs across the two subregions is about 3 gigawatts (GW), which is in line with current projects under construction (Network Development Plan [2019]).

<sup>5</sup>The decrease in marginal costs across the two regions is a form of the effect of transmission expansions on competitiveness as in Wolak [2015].

<sup>6</sup>One exception is Tangeras and Wolak [2019].

<sup>7</sup>Our paper is also related to the evaluation of different stringency levels of policies that incentivize the adoption of RES. Reguant [2019] compares Renewable Portfolio Standards (RPS) and FiTs focusing on the

The paper’s main objective is not an attempt to design the optimal structure of a FiT, but rather to quantify the benefits left on the table given its current structure. For example, [Stiglitz \[2019\]](#) identifies conditions for policies with differential pricing to be effective and [Abrell et al. \[2019b\]](#) showed that renewable energy support policies can be designed to be as cost efficient as a carbon price policy.<sup>8</sup> However, we show empirically that if the feasible solar penetration rate were used as a policy instrument for the allocation of solar capacity, there would be gains even when applying myopic optimization processes.

The paper is structured as follows. In [section 2](#) we describe the institutional background. In [section 3](#) and [section 4](#) we present the data and the marginal benefits. [Section 5](#) shows the misallocation results and the value of transmission capacity expansions. [Section 6](#) concludes.

## 2 Institutional Context

Germany was the first country to implement large-scale FiTs as part of the *Erneuerbare Energien Gesetz* (Renewable Energy Act) in 2000. FiTs can differ by installation size and type, but are otherwise uniform for each type of RES technology, not taking into account regional differences in sunshine radiation nor regional differences in electricity demand.

While the overall FiTs have decreased significantly between 2000 and 2017, mimicking the evolution of technology cost, the average FiT remains at about 30 euro-cents per kilowatt-hour (kWh) (see [Philipps and Warmuth \[2018\]](#)).<sup>9</sup> The large difference between costs for new installations and the average FiT stems from the fact that rates are set at the point in time when the installation is first connected to the grid and guaranteed for 20 years. Rates for PV systems depend on system size and mounting. While recent reforms of the Renewable Energy Act have led to the introduction of renewable capacity auctions, smaller residential

---

distributional implications of each policy. [Fell and Linn \[2013\]](#) compare RPS, production subsidies, and FiTs using a simulation model but without accounting for uncertainty. [Gowrisankaran et al. \[2016\]](#) estimate the welfare impacts of RPS for different levels of solar requirements but leaving aside FiTs. Other studies that focus on tax and subsidy policies in electricity markets include [Bahn et al. \[2020\]](#), [Borenstein \[2012\]](#), [Fowle et al. \[2016\]](#), [Knittel et al. \[2016\]](#), and [Leslie \[2018\]](#).

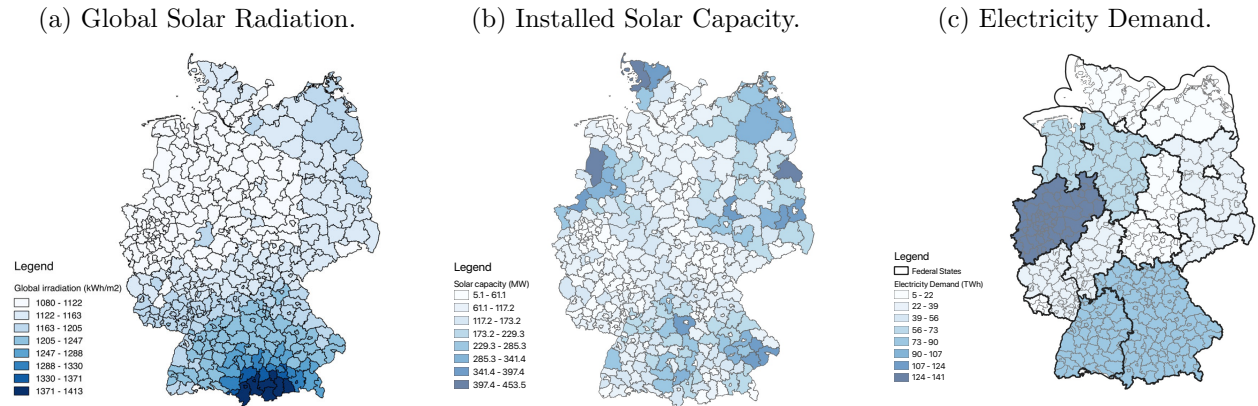
<sup>8</sup>See also [Wibulpolprasert \[2016\]](#). Similarly, [Ambec and Crampes \[2019\]](#) show that FiTs can be complemented with a price cap and capacity payments to obtain equivalent outcomes to a carbon tax.

<sup>9</sup>Figure D.1 in the Online Appendix plots the evolution of FiTs for solar systems of different size together with the average electricity price paid by the residential and industry sectors for the years 2000 to 2017.

installations continue to receive FiTs even after 2015.<sup>10</sup>

Figure 1 displays the total variation in sunshine radiation, installed solar capacity, and electricity demand in Germany. While there is clearly more solar radiation in Southern Germany, we find most of the installed capacity in North-West and North-East Germany.<sup>11</sup> An ideal policy would have likely led to a larger amount of installed solar capacity in the South. Figure 1c shows that total electricity demand –residential, commercial, and industrial combined– also varies across regions, but it does so without a good overlapping with solar radiation nor with installed solar capacity. The question is thus whether the dispersion in potential productivity of installations aligns with the dispersion in marginal benefits. If this is not the case, it is of interest to quantify the value left on the table from installing panels in regions with low solar productivity instead of installing more solar capacity in regions where the panels would be more productive and with higher benefits.

Figure 1: Regional Variation in Solar Radiation, Solar Installations and Electricity Demand



Notes: Global solar radiation (long-term averages) measured in kWh / m<sup>2</sup> in Panel 1a, cumulative solar capacity (Dec 2016) in Panel 1b, and electricity demand (2015) at state level in Panel 1c. Darker areas represent higher solar radiation, more installed capacity, and higher electricity demand, respectively. Data sources: German Weather Service, Official RES registry, and Statistical Offices of the German States, respectively.

<sup>10</sup>The timing of ‘entry’ of new PV plants is mainly related to the national FiT policy rather than regional factors. We confirm this by plotting the share of new solar installations in each region relative to the total number of solar installations within the corresponding TSO over the period 2000-16 and we do not find any evidence of regional differences in installation timing. These series of plots are available upon request.

<sup>11</sup>We provide the total solar capacity for residential installations ( $\leq 10$ kW) in the Online Appendix Figure D.2.

### 3 Data

Our primary data sources are publicly available data from the German electricity market. We obtain high-frequency data on load and supply from solar and conventional plants for each of the four regulatory zones that are served by one of the Transmission System Operators (TSOs) in Germany for the years 2015 and 2016. The four TSOs are 50Hertz, Amprion, TenneT, and TransnetBW. These data were obtained from the European Network of Transmission System Operators for Electricity (ENTSO-E) and are available at the 15-minute interval and for each type of production technology.

To calculate the daily electricity production costs by technology (coal, natural gas, fuel oil), we enrich these data with detailed fuel prices for Germany obtained from Bloomberg and official input-output tables from the working group on energy balances (AG Energiebilanzen) to determine the conversion factors from primary energy to electricity. These data allow us to calculate electricity production costs as well as emission factors by technology. We do not employ wholesale electricity price data because they do not necessarily reflect the cost of production as market power may be an important component of the observed price levels.<sup>12</sup> Instead, we obtain the marginal cost for each time period as described in the next section. Therefore, our results do not reflect issues related to market power in the wholesale segment.

We also use data on the type, quantity, and cost of ancillary services at the TSO level. These data are available from the official tender platform at 15-minute intervals and describe the procurement of secondary and tertiary control reserves. While system balancing takes place at the TSO level, there exists one common price for ancillary services in Germany.<sup>13</sup>

Figure D.3 in the Online Appendix plots the average portfolio mix by TSO for the years 2015 and 2016. This graph documents that there is great amount of heterogeneity across the

---

<sup>12</sup>Since the wholesale electricity price is uniform, it does not allow us to disentangle regional differences. TSOs are responsible for grid balancing in their area and congestion between the TSOs can lead to differences in marginal costs. We obtain electricity production (fuel) costs for other technologies that are not determined in a global market, such as lignite and nuclear from [ENTSO-E \[2018\]](#).

<sup>13</sup>We use the activated secondary control reserve, activated minute reserve and “balance exchange energy prices” (reBAP). While reBAP are labeled as prices by the operator, we will refer to them sometimes as costs in the absence of pure costs measures. We further focus on the ancillary services provided by the TSO and abstract from (international) grid control cooperation. See [Regelleistung \[2018\]](#).

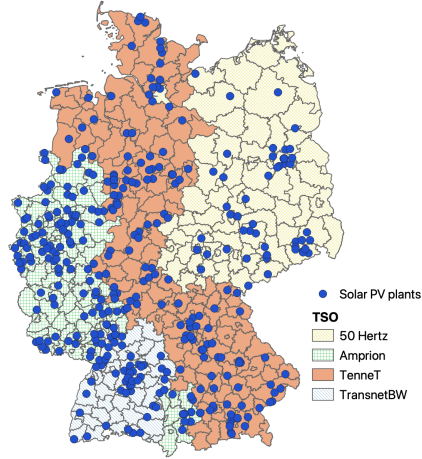
TSOs. While 50Hertz and Amprion have a large share of brown coal plants, TransnetBW has the largest dependence on nuclear. Our analysis focuses on one well-defined market and abstracts from imports and exports to Germany. The variability of net load over time even when aggregated at the national level and the diversity in the portfolio mix across the different TSOs, suggest that not only the marginal benefits in each of those regions can be different but also over time.

We complement the aggregate data at the TSO level with several disaggregated data sources. First, we obtain disaggregate data on all solar installations in Germany that are subject to FiTs.<sup>14</sup> We complement those data with solar PV production information from individual residential plants available from [PV Output \[2020\]](#), which provides us with the power produced at the PV station level at 15-minute intervals for a subset of all plants across Germany. More importantly, individual solar PV production data allow us to take into account plant heterogeneity in production (due to panel orientation, number and type of inverter, shading, etc.) and to have a distribution of solar PV output by TSO. [Figure 2](#) shows the four TSOs and the location of the individual solar PV production plants in our dataset. Second, we obtain data on the location, technology, and installed capacity of conventional power plants in Germany from Open Power System Data (OPSD) [[Neon Neue Energieökonomik et al., 2019](#)], which, in turn, are based on official statistics from the German Environmental Agency and the Federal Ministry for Economic Affairs and Energy. For all plants with an installed capacity of 100 MW or more, we furthermore obtain the history of plant unavailability and plant outages, which is available from ENTSO-E at the 15-minute interval. Moreover, to account for co-pollutants in our analysis, such as nitrogen oxides ( $\text{NO}_x$ ) and sulfur oxides ( $\text{SO}_x$ ), we combine the list of conventional power plants with plant-level pollution data from the European Pollutant Release and Transfer Register (E-PRTR). Further details are described in the Online Appendix A.2. Finally, we complement our dataset with regional statistics on population and economic output, as well as total energy demand, available at the county and state level, respectively, from the regional statistical offices in Germany.

---

<sup>14</sup>These data are available from the joint information platform of the four TSOs ([Netztransparenz \[2018\]](#)).

Figure 2: TSO Service Areas with Solar PV plants ( $\leq 10$  kW)



*Notes:* Each blue dot represents a residential solar PV installation ( $\leq 10$  kW) for which we observe electricity generation data at high frequency. Data obtained from [PV Output \[2020\]](#).

## 4 Quantifying the Marginal Benefits

We start our analysis by computing a measure of the value of an additional unit of electricity produced by RES. This is based on a combination of the short-term social and private costs associated with non-RES production. We separate the marginal benefits ( $MB$ ) from one unit of production of electricity from solar plants in region  $j$  and time  $t$  as:

$$\begin{aligned}
 MB_{jt} = & \text{value of displaced emissions}_{jt} \\
 & + \text{avoided operating costs}_{jt} \\
 & + \text{avoided ancillary service costs}_{jt}
 \end{aligned}$$

in a similar manner as in [Callaway et al. \[2018\]](#). The last term can also be negative as explained below. The first component captures the social costs and the last two the private costs. Our final goal from this part of the analysis is to compare the distribution of  $MB_{jt}$  against the uniform nature of the FiT incentive. We abstract from capacity markets as Germany is an “energy-only market”, in which only produced power is compensated.<sup>15</sup>

<sup>15</sup>See for instance the report by the [Federal Ministry for Economic Affairs and Energy \(BMWi\) \[2015\]](#), which argues against the introduction of capacity markets in a foreseeable future in Germany.

The avoided operating costs are the savings from the last MWh produced by the marginal plant that is no longer needed if RES output can replace it. Then, as pointed out in [Callaway et al. \[2018\]](#), the avoided operating costs can be expressed as a correlation of marginal costs and RES output. Let  $\lambda_{jt}$  be the marginal cost in region  $j$  at time  $t$  and let  $\omega_{jt}$  be the RES output at time  $t$  divided by the total RES production in a time interval  $[0, T]$ . Then, using the values of  $\omega_{jt}$  as the realizations of the probability density of the RES output we obtain that the average avoided operating costs per time period are

$$E[\text{avoided operating costs}_j] = \sum_{t=1}^T \omega_{jt} \lambda_{jt} = \bar{\lambda}_j + T \times Cov(\omega_j, \lambda_j),$$

where  $\bar{\lambda}_j$  is the expected value of  $\lambda_{jt}$  and we use the fact that  $\sum_t \omega_{jt} = 1$ . That expression makes clear that the weighted sum of marginal costs is the average of marginal costs in region  $j$  plus a term that depends on the correlation between marginal costs and solar output. The higher this correlation, the higher the value of avoided operating costs. Therefore, the geographical location of both the RES installation and the conventional sources is an important component of their value.

The same arithmetic applies to the case of emissions. Let  $e_{jt}$  be the emissions of the marginal plant at time  $t$  in region  $j$ . Then

$$E[\text{displaced emissions}_j] = \sum_{t=1}^T \omega_{jt} e_{jt} = \bar{e}_j + T \times Cov(\omega_j, e_j),$$

where  $\bar{e}_j$  is the expected value of  $e_{jt}$ . This shows that a positive correlation of emissions and RES output increases the value of the displaced emissions. Therefore, the correlations in both cases can be increased by inducing higher installation rates in regions with higher solar productivity, higher emitting plants, and higher marginal costs. In the next section we show the results both for CO<sub>2</sub> emissions alone and then including co-pollutants.

The ancillary services costs would follow a similar valuation if the marginal cost of this production were known. However, the typical data for this component are of a different nature and we propose a new approach to account for it in [subsection 4.2](#).

## 4.1 Avoided operating costs and emissions

For each 15-minute time interval  $t$  we sort the technologies by their marginal cost and form the perfectly competitive supply curve, i.e. the system’s marginal costs. Then we intersect that curve with the demand at time  $t$  and store the value of the marginal cost associated to the technology at that intersection. We call that marginal cost  $\lambda_{jt}$ , where  $j$  identifies the TSO. The underlying assumption is that load is dispatched by minimizing production costs.<sup>16</sup> Note that this assumption on the ranking of the technologies to be dispatched (merit-order) makes sense even in the presence of market power as long as there is not strategic withholding, which would clearly change the order of the dispatched plants. We elaborate on the detailed procedure in the Online Appendix A. There, Table A.1 shows the resulting simulated frequencies of the marginal technologies for the years 2015 and 2016 and here [Figure 3](#) the distribution of the marginal costs for each of the four TSOs. Consistent with other electricity markets, natural gas plants are the most frequent to be the marginal technology (62% of the time) followed by hard coal (36%) and then the rest of the technologies each with less than 2% of the time. The marginal costs distribution for TransnetBW is shifted to the left with respect to the other three TSOs in part because of its large share of nuclear capacity (the largest among the four TSOs).

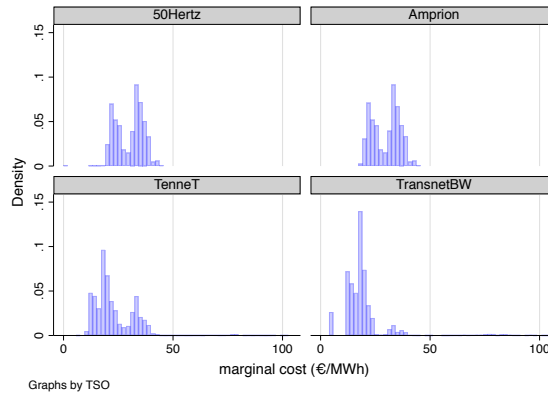
While Germany is separated in four TSOs, power plants bid into a common market with a uniform spot price. Yet, in our analysis we refrain from using spot prices and model TSOs independently and thus allow for the possibility that marginal technologies are heterogeneous across regions. As a robustness check, we recalculate a “common merit-order” case, in which we pool all TSOs (see the Online Appendix A.1) and we use it in the main misallocation analysis in [section 5](#).

Since we stored the identity of the marginal technology for each time interval, we can also compute the avoided emissions from those marginal plants. Then we use a social cost of carbon (SCC) of 31.71 €/tCO<sub>2</sub> as our baseline valuation to transform these emissions

---

<sup>16</sup>We make the implicit assumption that each TSO balances demand and supply independently and that there is no interconnection between the entities. We relax this assumption in [subsection 5.3](#).

Figure 3: Distribution of Marginal Operating Costs by TSO



*Notes:* Each panel shows the histogram of  $\lambda_{jt}$  for a given TSO  $j$ .

into euros per MWh.<sup>17</sup> We show the summary statistics of the avoided emissions multiplied by our baseline SCC value in the fourth column of [Table 1](#). We also consider two higher values for the SCC, 50 and 100 €/tCO<sub>2</sub>, which correspond to the two scenarios in [Abrell et al. \[2019b\]](#) and are similar to those in [Gillingham and Ovaere \[2020\]](#). All of our results are obtained using an SCC value of 31.71 €/tCO<sub>2</sub> unless otherwise specified, which is on the conservative side of RES valuations.

The introduction of the Renewable Energy Act (FiT) in 2000 had for objective to “allow for a sustainable development and energy provision in the interest of climate and environmental protection”. More precisely, to increase the share of RES in electricity generation (at least double until 2010). One of the main driving forces behind the law were the commitments related to the Kyoto agreement (to reduce greenhouse gas (GHG) emissions by 21% until 2010).<sup>18</sup> Therefore, one interpretation is that the original objective of the FiT policy was to address only GHG emissions (CO<sub>2</sub>). However, for completeness, we extend

<sup>17</sup>The SCC is designed to measure climate change damages and includes effects on human health, agricultural output, property damages from flood risk, and changes in heating and air-conditioning costs ([EPA \[2016\]](#)). We chose the SCC in the US of 36 \$/tCO<sub>2</sub> at a discount rate of 3% annual for year 2015. This value is equivalent to 31.71 €/tCO<sub>2</sub> using an average of the exchange rate between the two currencies of 0.88 dollars per euro. The last two times this exchange rate applied were at the end of December 2019 and at the end of March 2020.

<sup>18</sup>See [Ministry of Economy and Energy \[2000\]](#) for the regulatory document as well as a discussion on the motivation for the introduction of the original Renewable Energy Act (EEG 2000).

our analysis to account for major co-pollutants,  $\text{NO}_X$  and  $\text{SO}_X$ . Using monetary values for the damages per ton of these pollutants, we present an additional set of results from our reallocation algorithm that includes these co-pollutants together with the  $\text{CO}_2$  emissions. To carry this out, we collected additional data on emissions of  $\text{NO}_X$  and  $\text{SO}_X$  using the same method as in [Jarvis et al. \[2022\]](#).<sup>19</sup> A detailed description on these data and their treatment can be found in the Online Appendix A.2.

## 4.2 Ancillary services costs and solar output

The third component in our marginal benefits calculation has received little attention in the literature. One exception is [Tangeras and Wolak \[2019\]](#) who use a kernel regression to find the effect of solar output on ancillary costs in California. Their results show that the effect can change signs depending on the amount of load and solar output. We opt for a new approach to estimate this effect that will allow us to reduce the computational burden of our reallocation simulations in the next section.

Ancillary services have for objective to lower or increase the system’s electricity output if there is a misalignment between supply and demand that could destabilize the system. In Germany, there are three types of ancillary services (also known as reserves): primary, secondary, and tertiary. Primary reserves are relatively constant over time and tender calls are symmetrical, meaning that there is no separate call for positive and negative frequency containment reserves. In addition, these reserves are automatically activated by the ENTSO-E and they represent less than 10% of the volume of reserves.<sup>20</sup> Because of this, we do not use primary reserve costs in our calculations. Secondary and tertiary reserves, on the other hand, are provided and activated by the TSOs and market participants must submit two-part bids together with the respective prices for whether they can offer to increase or decrease their load level ([Furtwängler and Weber \[2019\]](#)). To the best of our knowledge, there are no reliable estimates of markups in the ancillary services markets, therefore we use the prices as a proxy for the costs ([Pollitt and Anaya \[2020\]](#)). The joint TSO internet platform on

---

<sup>19</sup>We thank Stephen Jarvis and Akshaya Jha for their helpful description of this data collection.

<sup>20</sup>See [Next Kraftwerke \[2020\]](#).

ancillary services defines this price as the ratio of net costs and the net balance position.<sup>21</sup> From that definition we can solve for the costs as

$$\begin{aligned} \text{ancillary costs}_{jt} = & \text{reBAP}_t \times (\text{SCR positive}_{jt} - \text{SCR negative}_{jt} + \\ & \text{MR positive}_{jt} - \text{MR negative}_{jt}), \end{aligned}$$

where the  $\text{reBAP}_t$  price is the uniform imbalance price (Bilanzausgleichsenergiepreise) at time  $t$ . SCR is the secondary reserve amount and MR is the minute-reserve or tertiary reserve amount in TSO  $j$  at time  $t$ . Therefore, the variability of the ancillary costs across different TSOs is due to the variability in the reserve amounts across the TSOs at a given point in time.

Our approach consists of estimating the relationship between the ancillary costs and the solar output and load through a linear regression of a polynomial that includes all the terms up to degree three (including interactions) as follows

$$\begin{aligned} \text{ancillary costs}_{jt}(S_{jt}, Q_{jt}) = & a_0 + a_1 S_{jt} + a_2 S_{jt}^2 + a_3 S_{jt}^3 + a_4 Q_{jt} + a_5 Q_{jt}^2 + a_6 Q_{jt}^3 + \\ & + a_7 S_{jt} Q_{jt} + a_8 S_{jt} Q_{jt}^2 + a_9 S_{jt}^2 Q_{jt} + FE. \end{aligned}$$

where  $a_i$  are the parameters to estimate,  $S_{jt}$  is the solar output and  $Q_{jt}$  is the total load at time  $t$  in TSO  $j$ . In addition, we include two-way fixed effects  $FEs$  of hour of the day, day of the week, month, and year. The marginal effect from an increase in renewable output on expected ancillary services costs is the derivative of the expression above with respect to  $S_{jt}$ .

We can estimate that specification by pooling all the observations for which the solar output is positive (Online Appendix Table B.1 and Table B.4). However, in order to distinguish the different effects that high load levels may have on ancillary costs relative to the effects when demand is low, we also estimate the same regression conditional on different levels of load. Inspired by the clustering procedures used by [Reguant \[2019\]](#), [Bahn et al. \[2020\]](#), and [Green et al. \[2011\]](#), we segment our sample into three different load profiles separately in each TSO using the  $k$ -means clustering method and estimate the polynomial regression above at

---

<sup>21</sup>See [Regelleistung \[2020\]](#). Note that the reBAP can take on both positive and negative values for each time interval and it is mostly based on costs of balancing energy but not capacity costs.

each of the twelve subsamples.<sup>22</sup>

We present the regression results in Table B.2 and Table B.3 in the Online Appendix. We find that a large number of the individual coefficients in each of the regressions is statistically significant and that the coefficients have stark differences across the different load profile clusters. In our counterfactual simulations, we use directly the values of those coefficients in the expressions for  $\frac{\partial \text{ancillary costs}_{jt}}{\partial S_{jt}}$  to obtain ancillary services costs at different combinations of solar output and load. However, to provide an intuitive interpretation we evaluate the derivative, using the estimated coefficients, at each time interval and then obtain the mean of those values, which range from  $-1.06$  to  $2.45$  €/ MWh, see Table B.5 in the Online Appendix.<sup>23</sup> Overall, we obtain highly state-dependent responses of ancillary services costs, a finding that is in line with [Tangeras and Wolak \[2019\]](#).

### 4.3 Total marginal benefits

The total expected value of the marginal benefits are shown in [Table 1](#). The first *Total* column, Column (5), does not include co-pollutants and the second *Total* column, Column (8), adds them. As pointed out in the computation for each of the components of the marginal benefits, there is a different value at each 15-minute interval and for each TSO. To simplify the exposition of these results we opt for showing the simple arithmetic means and the standard deviations only. There are several things worth noting. First, in the case of CO<sub>2</sub> emissions only, the avoided operating cost accounts, on average, for between 45% and 72% of the total marginal benefits. Second, the marginal effect of ancillary services with respect to solar is small compared to the other two components. However, these are non-negligible amounts in the aggregate and the average values can be costs or benefits depending on the TSO, but with high volatility. The fact that increasing RES can lower ancillary service costs is supported by the overall time trend. While over the time period 2008 to 2015 wind and solar capacity have augmented roughly by 200% in Germany, the total amount of balancing

---

<sup>22</sup>Further details can be found in the Online Appendix B.

<sup>23</sup>Alternatively, we can evaluate the derivative at the mean of load for each TSO and cluster to obtain a function of solar output, see the Online Appendix Figure B.2.

reserves has decreased by 20%.<sup>24</sup> Finally, our results show heterogeneity for the four TSOs as measured by the standard deviations of the marginal benefits. Once we add the co-pollutants to the marginal benefits, the ranking of the four TSOs only changes between the third and fourth place (a difference of 0.14 €) and the percentage difference between the highest and the smallest mean marginal benefits relative to the highest marginal benefit is 25.4% instead of 8.4% from the case of no co-pollutants. In other words, whilst the degree of heterogeneity increased with the inclusion of the co-pollutants, the ranking of the TSOs remains highly comparable.

Table 1: Expected Value and Standard Deviation of Marginal Benefits

TSO	MB without co-pollutants				MB with co-pollutants		
	Anc. costs	Op. costs	CO <sub>2</sub>	<b>Total</b>	SO <sub>x</sub>	NO <sub>x</sub>	<b>Total</b>
Amprion	-0.82 (3.01)	29.39 (6.3)	12.48 (2.09)	41.05 (6.80)	0.38 (2.15)	0.56 (0.12)	41.99 (7.36)
TenneT	0.48 (1.31)	21.97 (10.14)	22.34 (7.28)	44.79 (8.46)	10.38 (7.56)	1.11 (0.41)	56.28 (11.43)
TransnetBW	0.22 (3.39)	19.34 (13.02)	23.2 (7.58)	42.76 (16.08)	12.03 (6.25)	1.16 (0.42)	55.95 (17.75)
50Hertz	-0.49 (2.18)	29.37 (6.39)	12.13 (1)	41.01 (6.85)	0.58 (0.89)	0.54 (0.05)	42.13 (6.93)

*Notes:* All numbers in €/MWh. Columns (2) to (5) show the averages and standard deviations (in parentheses) of each of the components of marginal benefits (MBs) and the total without considering co-pollutants. Negative avoided ancillary costs represent costs, while positive values represent gains. The last three columns contain the average marginal benefit and standard deviation (in parentheses) from co-pollutants and the overall totals. Each outcome presented by TSO.

## 5 Measuring Misallocation

In this section we measure the misallocation resulting from the current solar panel installations locations using our estimates for the marginal benefits and an optimization process. To ease the exposition of our results we focus on the case of CO<sub>2</sub> emissions without co-pollutants. This is motivated by two reasons: (i) a straightforward interpretation of the Renewable Energy Act is that the FiT policy is concerned primarily with CO<sub>2</sub> emissions,

<sup>24</sup>See [Hirth \[2015\]](#).

and (ii) as explained in the previous section, the inclusion of the co-pollutants does not alter substantially the ranking of the TSOs regarding benefits. We report on the reallocation analysis with co-pollutants in the Appendix.

We exploit the heterogeneity in regional solar radiation and marginal benefits to calculate a counterfactual allocation of solar installations in Germany so that every incremental amount of solar capacity to be reallocated is placed where the resulting benefits are the highest. We focus on small scale residential solar installations in [subsection 5.1](#) and on all solar capacity in [subsection 5.3](#). We compare this counterfactual allocation’s output and total benefits to the output and benefits from the actual location of PV installations. Our measure of misallocation is the ratio of the total benefit values from each scenario, where the value is based on the expected marginal benefits of solar in each region.

## 5.1 Reallocating RES

We start by computing the value of the actual solar allocation: each unit of observed solar output is valued at the  $MB_{jt}$  (different every 15-min in each TSO). We recognize that  $MB_{jt}$  is a non-constant function of the solar output, which accounts for the different displacement effects from high and low levels of the feasible solar penetration rate. Then we take the sum over our entire sample period. This is the baseline value used below to compute the gains of each reallocation scenario. Note that this value takes into account both differences in solar productivity and differences in  $MB$  across regions and time periods.

In our policy experiments we impose as a constraint that the counterfactual installation of solar PV on residential buildings cannot exceed a certain penetration rate. We call it the *feasible solar penetration rate* (FSPR henceforth) and we denote it by  $\gamma$ . At an FSPR of 100% ( $\gamma = 1$ ), all feasible residential buildings in a given area would have solar panels installed on their rooftops. We calibrate this parameter using data from 2016. That year the FSPR is approximately 5%.<sup>25</sup> In line with the average size of residential solar installations in Germany, we assume a capacity of 6.7 kW per rooftop. The total number of residential

---

<sup>25</sup>We calculate this value at the TSO level for the last month of our sample, December 2016, using the housing stock from the 2011 census. If using county level data instead, we find an average of 6% with an interquartile range between 3.3% and 8.2%.

buildings varies from 2.2 million in TransnetBW up to approximately 7 million in the largest TSO, TenneT.<sup>26</sup>

For each of the reallocation scenarios we consider an FSPR greater or equal to 5% and each TSO is subject to the same rate for any given scenario. Since we are interested only in measuring misallocation of resources, we keep the total solar capacity fixed throughout our different scenarios.

We now describe how we optimize the reallocation of solar capacity. Let  $\mathcal{C}$  be the total amount of currently installed residential solar capacity in all the TSOs together. Split  $\mathcal{C}$  into discrete blocks of capacity of size  $c$  each (for example  $c = 1$  MW). For a given value of the FSPR  $\gamma$  we reallocate  $\mathcal{C}$  as follows, starting with zero cumulative capacity in each TSO:

1. Add a block of capacity of size  $c$  to the cumulative solar capacity in each TSO.
2. For each TSO separately, compute the expected gains from adding the amount  $c$  to the TSO's capacity.
3. Compare the gains in each of the TSOs and permanently allocate the capacity  $c$  to the TSO for which total gains are the largest if the fraction of the cumulative solar capacity in this TSO with this addition is less or equal to  $\gamma$ .
  - In case no more capacity can be added to the TSO with the highest value, i.e. we have reached the FSPR, allocate  $c$  to the TSO with the second highest gains.
  - Similarly, in case the FSPR is binding for the TSO with the second highest gains, move to the TSO with the third highest gains, and so on.
4. If  $\mathcal{C}$  has not been completely reallocated, go back to step 1. Otherwise, the process ends since there is no more capacity to reallocate.

In order to determine where to allocate the next block of capacity  $c$ , we must compute the gains in each TSO and choose the TSO where those gains are the largest. This process

---

<sup>26</sup>The FSPR can be interpreted as a type of Renewable Portfolio Standard (RPS). However, instead of a mandate on the fraction of load to be covered by RES production, we define  $\gamma$  as a fraction of maximum potential capacity.

exhausts all the possibilities of allocation, conditional on the size  $c$  of the blocks. The configuration we find at the end of this process is optimal because we obtain the configuration by construction.

We use the TSO-specific  $MB_{jt}$  and data on residential solar production at the 15-min interval to multiply the newly allocated solar capacity in each TSO at each step of the algorithm to convert capacity (MW) into production (MWh) and ultimately into a monetary value (€/MWh). The algorithm thus accounts for both regional *differences in solar productivity* and *differences in the marginal benefits* from solar production. As the cumulative amount of solar increases in the TSOs, the value of the marginal benefits changes since it is possible that the conventional technology displaced is of a different nature than when the first block  $c$  was allocated. Our three components of marginal benefits can take on different values as the cumulative solar capacity increases or decreases relative to the actual allocation. When the solar capacity in a TSO is lower relative to its initial amount –as it can happen when in a step of the algorithm the marginal benefits for that block are greater elsewhere—we use the value of  $MB_{jt}$  from the actual allocation. That is, we assume the  $MB$  function to be constant for solar rates that are lower than the initial rate in the TSO. However, if the cumulative solar capacity is greater than its initial amount, there is displacement of conventional sources of production and we invoke our  $MB$  function which evaluates the effects from this displacement in terms of avoided operating costs, avoided emissions, and avoided ancillary costs.<sup>27</sup>

Although unlikely, if solar output from residential installations were enough to cover total load in the TSO, only the units needed to satisfy demand would be valued at the  $MB$ s since the surplus would not displace any traditional technology. This never occurs during our sample period.<sup>28</sup> When we reallocate also larger solar installations, we introduce the possibility of transmission in [subsection 5.3](#). In this case, the surplus will be valued at the  $MB$  of the importer of this excess.

In addition, we consider two variations to the algorithm described above.

---

<sup>27</sup>Using this procedure, we can rely directly on data as opposed to simulated supply curves.

<sup>28</sup>Even if all solar were allocated to the TSO with the highest  $MB$  (TransnetBW), the production from residential installations would only account for 15% of total load on average (maximum of 74%).

**Irradiation ranking.** In the previous setting, we aim at quantifying the total level of misallocation resulting from both differences in solar radiation *and* differences in marginal benefits across regions. In terms of policy design, the policy maker does not know the distribution of marginal benefits ex-ante. In order to separate the two effects, we reestimate the reallocation gains, assuming that the only information available to the decision maker is the observed average solar radiation per region. Table D.2 in the Online Appendix shows the average solar productivity per TSO obtained through linear regressions of individual solar plant-level production data on installation characteristics. The TSO-specific coefficients measure the average productivity of the PV sites in each TSO. All other parameters as well as the calculation of the total benefits remain unchanged. This naive optimization process allocates as much solar capacity as possible (up to a fraction  $\gamma$ ) in the most productive TSO, then it reallocates the remaining solar capacity in the second most productive TSO (up to a fraction  $\gamma$ ), and so on until total initial solar capacity is reallocated. This process gives a suboptimal solution because the *MB* function for the most productive TSO might decrease quickly with the addition of solar capacity, and some of the capacity could contribute with more gains if placed in a TSO where the *MB* is higher instead even if productivity is slightly lower.

**Common merit-order.** Since there is a common electricity market in Germany with a uniform spot price, a potential concern is that the relevant marginal technology is the one that determines the spot price and not the marginal source in each TSO separately. Therefore, we provide a robustness check for our main results consisting of the use of a common merit-order curve, i.e. while each TSO can have a different solar productivity, the MBs are constant across the four TSOs. We elaborate on the detailed aggregation procedure in the Online Appendix A.1.

The results from each of the three optimization processes consist of reallocating residential solar installation plants assuming an FSPR ( $\gamma$ ) of at least 5%.<sup>29</sup> Very low values of  $\gamma$  would

---

<sup>29</sup>There is some heterogeneity in the observed FSPR in 2016: 50 Hertz 2.3%, Amprion 4.3%, TenneT 4.8%, and TransnetBW 7.4%. Therefore, by assuming  $\gamma = 5\%$  there is still some reallocation happening, i.e., some capacity will be reallocated from TransnetBW (most productive area) to another area with higher marginal benefits but less productive.

imply that  $\mathcal{C}$  is not fully reallocated among the four TSOs, leaving a fraction of  $\mathcal{C}$  unused, which would result in an inefficient allocation.

Our main outcome of interest is the ratio

$$\text{Reallocation value at } \gamma = 100 \times \left( \frac{\text{value of reallocated solar capacity at } \gamma}{\text{value of current allocation of solar capacity}} - 1 \right) (1)$$

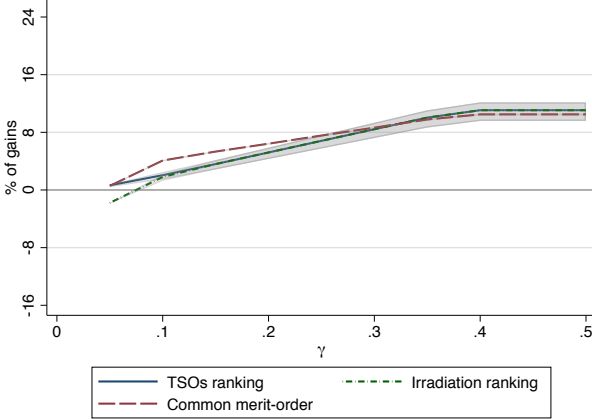
where the numerator inside the parentheses changes as we allow for a larger FSPR but the denominator is fixed and corresponds to the observed configuration. Therefore, when  $\gamma$  is small, we should have gains close to 0. [Figure 4](#) shows the reallocation gains expressed as percentages and the same gains in levels for different values of the FSPR and of the SCC. To facilitate the presentation of our results we start with the case of our baseline algorithm, labelled “TSOs ranking” in that same figure.

As the FSPR ( $\gamma$ ) increases, more of the existing solar capacity gets allocated to the regions with higher marginal benefits, until the gains become flat at approximately  $\gamma = 40\%$ , when all solar capacity gets allocated to the most productive TSO. Since we focus on residential installations in this section, solar output is typically not large enough to displace all load in a given TSO. By using larger values for the SCC, the benefits curve becomes steeper at low and medium values of the FSPR and leads to larger gains for all values of  $\gamma$  considered. The only case where we observe smaller gains is for the lowest value of  $\gamma$  and an SCC value of 100 €/ MWh. This is due to the particular portfolio mix and related emissions of the TSOs that receive more solar capacity than their initial amounts. Yet, also in this case the gains increase with the FSPR.

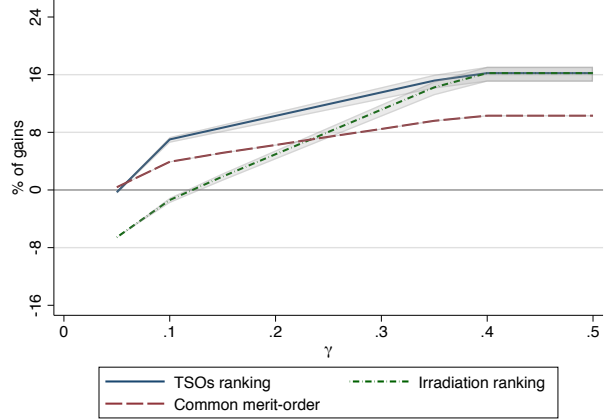
To provide a measure of uncertainty of our main results, for each value of  $\gamma$  we compute the gains from reallocation using load and solar output observations that are increased by two standard deviations computed from the joint distribution of residuals of a seemingly unrelated regression of load and solar output. Then we repeat but decreasing each of load and solar output by two standard deviations of the residuals distribution. More specifically, we regress load on its 1-hour lagged value and its 24-hours lagged value together with TSO, hour of the day, day of the week, month, and year dummy variables. Similarly for solar output, where we employ the individual solar PV production data. We recover the residuals

Figure 4: Value of Reallocation for Different Values of SCC and  $\gamma$

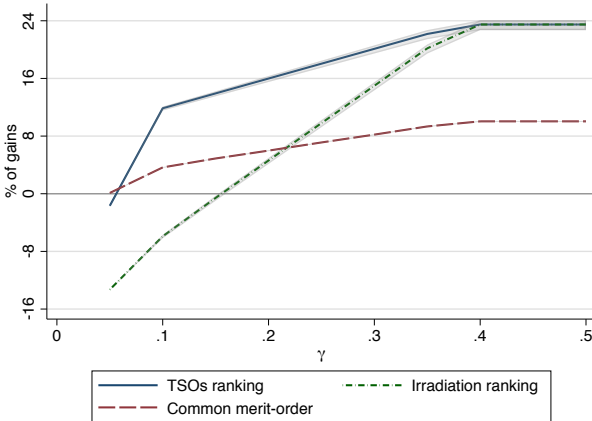
(a) SCC = 31.71 €/tCO<sub>2</sub>



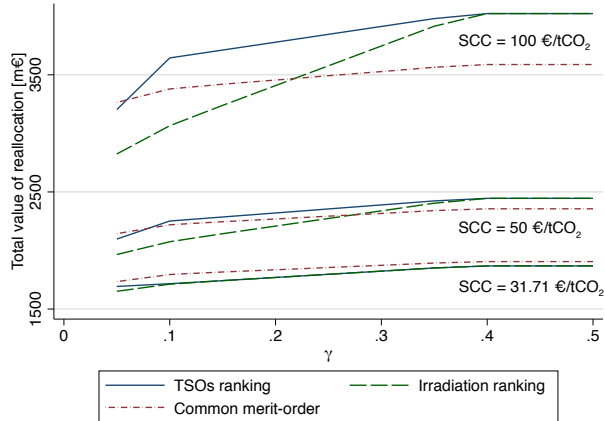
(b) SCC = 50 €/tCO<sub>2</sub>



(c) SCC = 100 €/tCO<sub>2</sub>



(d) Total value of solar under reallocation m€



*Notes:* Panels (a) to (c): Each line represents the value of reallocated solar capacity as defined in Equation 1. We report the gains for the optimal allocation using the TSO specific ranking (solid blue line), a TSO ranking that is only based on solar irradiation (dotted green line), and using a common-merit order dispatching (dashed red line). For each value of the FSPR  $\gamma$  we also compute the gains when adding and subtracting two standard deviations of the joint distribution of residuals from a seemingly unrelated regression of load and solar output (see main text for details). This produces the bands around the main outcomes and represent the uncertainty in the simulations. Panel (d) shows the total value of the reallocation (in million euros) for each of our values for the SCC and for each of the three variations of the reallocation algorithm. No uncertainty bands shown.

from this system of equations and calculate their standard deviations by TSO.<sup>30</sup> The bands around the main line in [Figure 4](#) represent the gains for combinations of an increase or a decrease on solar output or load by the same number of standard deviations of their respective residuals distribution. Consistent with the regressions on average solar productivity from the Online Appendix Table D.2, we see almost no uncertainty in the gains. This is mainly driven by the fact that residential installations in a given TSO are rather homogeneous and produce a similar output.

Our results show that with a solar rate of 20% the gains are 5.2% (avoided ancillary services + avoided production costs + avoided emissions) relative to the actual allocation and using our baseline value of the SCC, and 8.4% when  $\gamma = 30\%$ .<sup>31</sup> Those percentage changes may seem small. However, to put them in perspective, the increase in levels from the baseline to the reallocation configuration when  $\gamma = 0.2$  is 88 million euros and 142 million euros when  $\gamma = 0.3$ . The annualized amount for a 20% FSPR (44 million euros) is roughly equivalent to the production of 220,000 residential PV plants of average size valued at an average wholesale electricity price of 30.30 €/MWh during our sample period, and to 354,000 PV plants of the same capacity when  $\gamma = 0.3$ .<sup>32</sup> In 2016, there were roughly 950,000 residential installations in Germany, therefore these values from misallocation represent approximately 23% and 37% of the market value of the production of all residential installations, respectively.

Those results use a relatively conservative measure of the SCC. With a higher valuation of 50 €/tCO<sub>2</sub> as in the main specification in [Abrell et al. \[2019b\]](#) who compute the social costs of different policies to incentivize the adoption of RES, the gains from reallocation are 10.3% and 13.5% when  $\gamma = 0.2$  and 0.3, respectively. For a value of SCC of 100 €/tCO<sub>2</sub> those gains are 16 and 20.1% respectively and as shown in [Figures 4b](#) and [4c](#). The width of the uncertainty bands decreases with the SCC value because there is less uncertainty about the gains when one of the components is highly valued.

[Figure 4d](#) reports the total value of solar under reallocation. To get a sense of their

---

<sup>30</sup>The detailed results from these regressions are available upon request.

<sup>31</sup>[Sexton et al. \[2021\]](#) assume a maximum share of households to be covered with solar panels of 30%.

<sup>32</sup>To calculate this number we use the average installation size together with the average annual production in Germany from the Online Appendix Table D.2 of 984 kWh/kW and the average wholesale electricity price. We find an annual production value of roughly 200 € per installation and year.

magnitude compared to the cost of the policy (the subsidy), we multiply the simulated solar output (solar capacity  $\times$  average production in each TSO) by the amount of the subsidy, assuming that all installations were completed in the same year (2014) and that there was no self-consumption. Then the policy’s gains net of the subsidy and relative to our baseline scenario are positive for all SCC and  $\gamma$  values. Specifically, we find annual net gains of up to 50 million euros for the lowest SCC value. Larger SCC values yield higher net gains.<sup>33</sup>

Figure 4 also shows two additional lines in Panels (a) - (c): the ex-ante optimal reallocation gains from using only the solar irradiation ranking and the ex-post optimal reallocation gains from the common merit-order case. Panel (d) summarizes the total value of solar from each of the nine cases: for each value of the SCC considered and for each of the three variations of the reallocation algorithm. In all the cases, the gains are non-decreasing in  $\gamma$  and converge to similar values for a given SCC value. This gives us confidence that our results are robust to a variety of specifications. Note that the percentage gains show a slightly larger variability with increasing values of the SCC, in particular for the common merit-order case, as in this case the baseline value is different.

In Panel (a) of Figure 4, the gains from the three rankings considered coincide almost perfectly. As the SCC value is increased in Panels (b) and (c), the gains from the irradiation ranking are lower than in the baseline case until they converge once  $\gamma$  is greater than 0.4. Since in the irradiation version of the algorithm the differences in production and ancillary services are not taken into account, the negative gains for low values of  $\gamma$  show that the marginal sources displaced are not the ones with the highest emissions. This is a natural motivation to consider the differences in marginal benefits from solar production and not only differences in irradiation levels since each production source has different emissions levels. The two lines converge in our analysis since the two rankings coincide for the TSO with the highest productivity, but this would not necessarily be the case in a different market.

---

<sup>33</sup>Note that also the total subsidy cost (solar capacity  $\times$  average production in each TSO  $\times$  subsidy) is increasing in  $\gamma$  because the reallocation increases total solar output by placing more solar in regions with higher solar productivity. The policy’s net gains defined as

$$(\text{value in reallocation} - \text{value in baseline}) - (\text{subsidy in reallocation} - \text{subsidy in baseline}),$$

are increasing in  $\gamma$  and similar in shape to the curves in Figure 4d. See Figure D.8 in the Online Appendix.

The common-merit order gains have a slightly flatter growth profile than the baseline case, ending at a moderately lower value of gains than the baseline for an SCC value of 50 or larger. This is due to the two main differences of this algorithm with the baseline reallocation method. First, the common-merit order is equivalent to the baseline optimization constrained to using only one marginal cost curve for the entire system instead of four distinct marginal cost curves. If there are any efficiency gains to be exploited from differences in the marginal sources across the four TSOs, the common-merit order ranking cannot exploit such differences. Second, recall that the marginal cost curve used for the common-merit order case is not directly the horizontal aggregation of the four marginal cost curves of the TSOs, this inevitably creates differences between the two algorithms (see Table A.1 vs. Table A.2 in the Online Appendix).

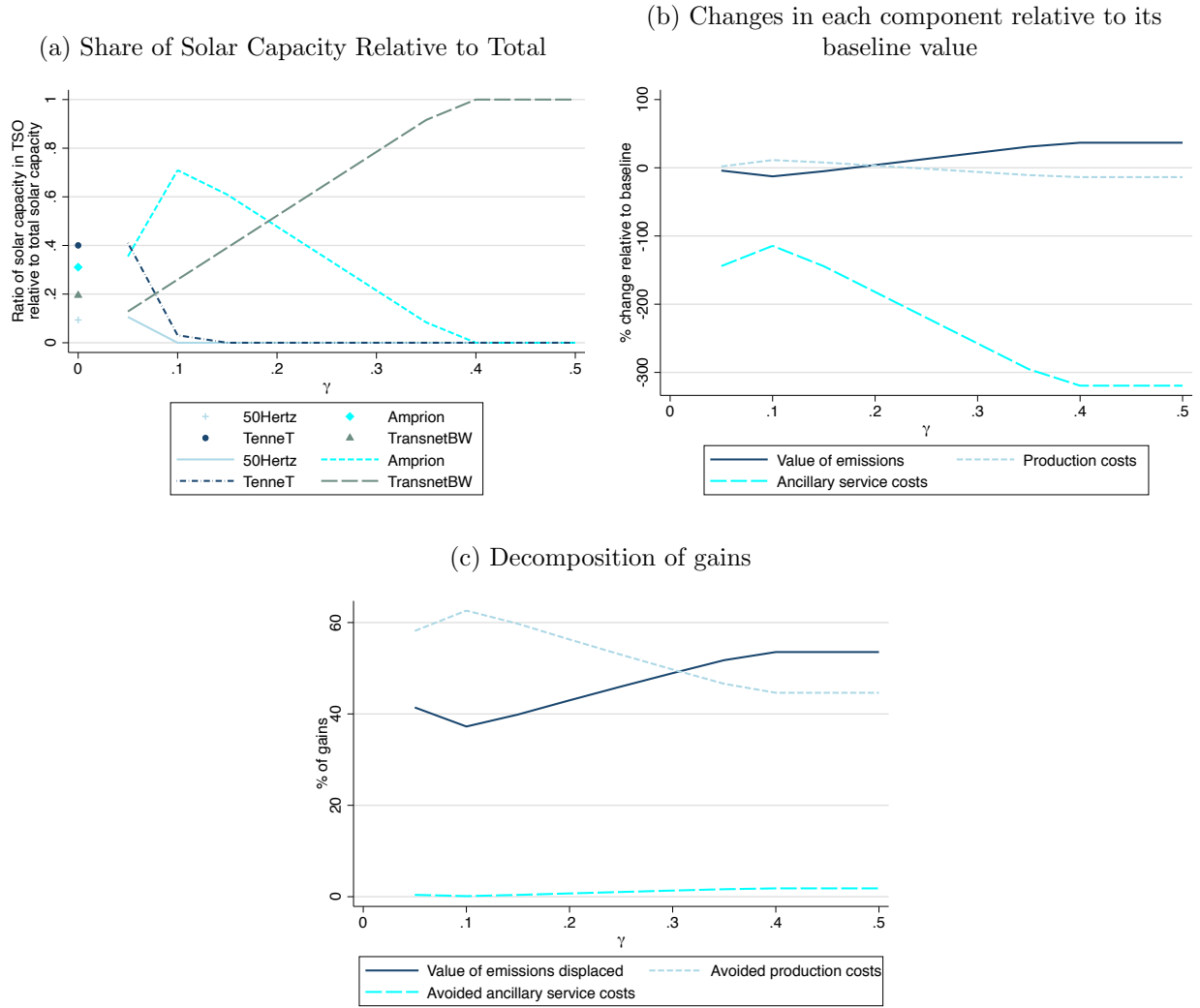
Finally, Online Appendix Figure D.4 summarizes the outcomes discussed in this section but for the case when the co-pollutants are included with the benchmark value of 31.71 €/tCO<sub>2</sub> for the SCC. Panel (a) in that figure shows that the gains from reallocation are very similar to the case without considering co-pollutants and with an SCC value of 50 or 100 €/tCO<sub>2</sub>. This suggests that including the effect of the co-pollutants is roughly equivalent to increasing the damage from CO<sub>2</sub> emissions by a factor between 2 and 3.

## 5.2 Capacity shares and decomposition of gains

Focusing on the case of the baseline algorithm, as more capacity goes to TSOs with higher marginal benefits, some TSOs end up without any solar capacity at all. This is shown in Figure 5a, which plots the shares of solar capacity in each TSO relative to the total solar residential capacity in Germany (not to be confused with the FSPR definition) at different values of  $\gamma$ . The figure also depicts the actual shares as points at  $\gamma = 0$ . For sufficiently high values of the penetration rate  $\gamma$ , there is a TSO with a share of 1.

While the total gains in Figure 4 are the net result of the combined changes in each of the three components of the marginal benefits, Figure 5b compares the percentage changes relative to their benchmark values of each of those components at each value of  $\gamma$  and Figure 5c shows the share of the contribution from each of the components (production costs,

Figure 5: Changes Relative to Baseline and Decomposition of Gains



*Notes:* Panel (a): Increases in the FSPR  $\gamma$  allow for a higher reallocation of solar capacity in the best regions while lowering the reallocation amount to the worst regions. This occurs because total solar capacity remains constant. Markers at  $\gamma = 0$  are the actual shares of solar capacity (residential solar installations  $\leq 10\text{kW}$ ) before any reallocation. Panel (b): For each component we compute the difference of its value at each level of  $\gamma$  and expressed it as a percentage relative to the value of that component before any reallocation. Negative percentage changes in ancillary service costs represent savings. In levels, these are small amounts. Panel (c): At each value of  $\gamma$ , we compute the fraction of the value of each component relative to the total gains and express it as percentage.

emissions, and ancillary services) to the total gains. For small values of the solar rate, the value of the emissions decreases relative to the baseline (negative sign) because some of the reallocated solar capacity no longer offsets high level emissions marginal plants in some TSOs. This is in line with the fact that large values of the SCC can lead to negative gains at low levels of  $\gamma$  in Figure 4. As the FSPR increases, the size of this displacement is larger than the total value of offset emissions from the baseline even in low-emitting TSOs. This is consistent with the portfolio mix of technologies by TSO shown in Online Appendix Figure D.3 and with the frequencies of marginal technologies in Online Appendix Table D.1. For example, the marginal technology in TransnetBW is dominated by hard coal, a high-emitting source, and according to Figure 5a, at  $\gamma = 0.05$  this TSO receives less solar capacity than in the actual allocation. Consequently, at these low levels of  $\gamma$ , other TSOs with a slightly cleaner production mix receive a larger share of solar capacity and the initial “gains” are negative. This, however, changes quickly as more capacity gets allocated to TransnetBW. Recall that the gains do not depend on the average technology mix within each TSO, which is dominated by nuclear in the case of TransnetBW, but on the marginal technologies displaced by adding solar to the system.<sup>34</sup> The negative gains in emissions are compensated by larger gains in production costs. For larger values of  $\gamma$ , the values of displaced emissions are, however, the most important component for the benefits. Finally, while ancillary service costs can decrease considerably with  $\gamma$ , their total impact on gains remains small, as highlighted in Figure 5c.

Figure 5b also highlights the trade-off a regulator (social planner) would face when reallocating solar capacity between evaluating the misallocation using a global measure of benefits as in our main results versus using only one of the components. For example, if the regulator cares only about maximizing the value of emissions displaced, the best value for  $\gamma$  would be any value above 0.4, as Figure 5b suggests. Similarly, if the objective was to decrease production costs only, the policy would require  $\gamma$  to be at least around 23% so that the

---

<sup>34</sup>Similarly, the relatively high frequencies of hard coal being the marginal technology should not be confused with the fact that natural gas powered-plants have higher marginal costs. The frequencies shown in Table D.1 in the Online Appendix are obtained by solving for the perfectly competitive equilibrium in each time period and low levels of net load intersect some of the TSOs marginal cost curves at the hard coal production segments more often than at the natural gas plants. This has been documented by market analysts (see [Timera Energy \[2014\]](#)).

changes in production costs relative the baseline are negative as shown in Figure 5b. As for the ancillary services, any value of  $\gamma$  considered decreases the costs, even beyond their initial amount.

Figure 5c shows the changes in the contribution of each component to the total gains. The figure makes evident that the two main drivers of the benefits are the value of emissions displaced and the savings in production costs, consistent with Table 1. Each of these components account for roughly 40 to 60% of total gains. The savings in ancillary services costs are much smaller.

Overall, similar results prevail in the case of the two variations of our baseline algorithm. Even in the common-merit order case, there is a reallocation of capacity that can be tracked for each TSO. Qualitatively, the results in this subsection are similar to those from the other two algorithms.<sup>35</sup> As for the case when including co-pollutants, the solar capacity shares and the decomposition of gains are shown in Panels (c) and (d) of Online Appendix D.4. In line with the main results with co-pollutants from Table 1, the figures make clear that the benefits from co-pollutants behave similarly to those from the avoided CO<sub>2</sub> emissions.

Our reallocation results show that in the presence of a flat incentive for solar PV adoption, the addition of a FSPR could have increased the gains stemming from the savings of displacing conventional sources of electricity and the value of the associated emissions avoided.<sup>36</sup> The actual implementation of such a policy is beyond the main scope of this paper.

### 5.3 The value of transmission

The increasing penetration of RES makes transmission lines more valuable and future investment in the transmission grid indispensable. This is especially true for large-scale RES installations, such as solar farms. Differences in the availability of RES energy paired with regional differences in expected energy demand growth led to the creation of the German

---

<sup>35</sup>These results are available upon request.

<sup>36</sup>The design of these policies could include a revenue-neutrality constraint in which the tax revenue from emissions equals the total amount spent in subsidies (for example, see Durrmeyer and Samano [2018]). We abstract from this and focus on the costs/benefits from the geographical dispersion.

*Network Development Plan* (NDP) in 2012.<sup>37</sup> Key projects discussed in the NDP are several high-voltage direct current lines between North and South Germany (see Online Appendix Figure D.5) with the objective to increase interchange capacity for electricity from RES production across regions. In particular, the NDP foresees different scenarios for increasing solar capacity investment in Southern Germany, as well as the development of wind farms in Northern Germany. While there are clear benefits from an increased interconnection of these regions, power line expansions have been largely criticized by the public based on their cost and potential environmental and aesthetic impacts.<sup>38</sup> Total investment costs for these large-scale transmission lines are highly project-specific.

We contribute to this ongoing policy debate on the value of transmission, by focusing on a single TSO, TenneT, which stretches from North to South Germany and that has large heterogeneity in solar productivity. In a counterfactual analysis, we split TenneT into two independent entities, and repeat the calculation of the marginal benefits from solar in each of these areas. In a second step, we perform a reallocation focusing on all solar capacity in Germany and allowing for different degrees of transmission capacity between the two areas to determine the value of transmission. We focus on *all* solar capacity rather than purely residential installations in this subsection to highlight the role of the transmission constraint, which is mainly relevant when there is excess energy production in one subregion. In a final step, we compare the additional benefits from the interconnection to the total investment cost for different cost scenarios.

We split TenneT into a North and South regions based on administrative boundaries.<sup>39</sup> We start our analysis by constructing the expected *MBs* for solar in the two regions. As load and electricity production data are only available at the TSO level, we construct demand

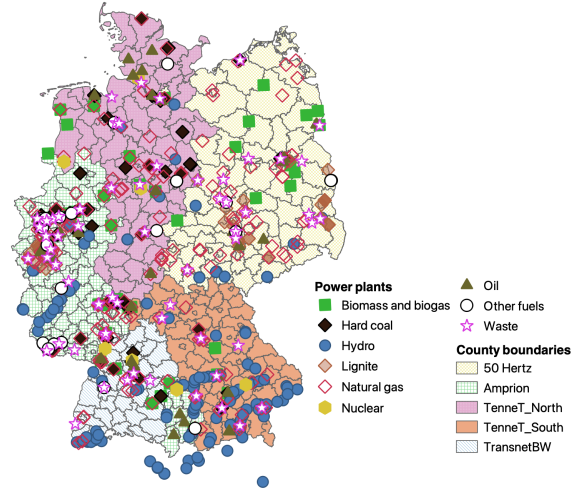
---

<sup>37</sup>Several revisions to the original NDP have been made in recent years. We consider here the 2019 version, which focuses on the electricity market in 2030 ([Network Development Plan \[2019\]](#)).

<sup>38</sup>Two key projects are Suedlink and SuedOstlink, both planned as direct current large-scale regional interconnections from North to South Germany with an approximate length of 730 km and 580 km, respectively. The projects encountered stark opposition by citizens' groups, which led to a re-evaluation of the power lines and the decision to implement them as underground lines. The total cost for these projects are estimated to be 10 billion euros (Suedlink) and 5 billion euros (SuedOstlink) ([Tennet \[2020a\]](#)).

<sup>39</sup>To split the TSO, we overlap the TSO area with state boundaries and use the state of Bavaria to define the South region within TenneT. Bavaria represents roughly half (46%) of the gross domestic product and about 41% of total population in TenneT.

Figure 6: TSO Service Areas and Conventional Power Plants



*Notes:* TenneT is split into North and South regions defined by the administrative boundaries of Bavaria. Each symbol represents a conventional power plant. Markers outside the Germany boundaries correspond to hydro power plants under control of one of the TSOs. Data obtained from OPSD [Neon Neue Energieökonomik et al., 2019].

and supply in the two subregions.<sup>40</sup> Using the exact geo-location for each plant in TenneT we assign them to the North or South region and assume that their output is predominantly used in that region (see Figure 6 for conventional power plants). Further information on the specific data sources and the construction of the supply curves for the two new regions can be found in the Online Appendix A.4.

Similar to the residential reallocation, for a given value of  $\gamma$ , we optimize for each MW of reallocated capacity according to the maximum expected benefit calculated as solar production  $\times MB_{jt}$ , where both solar productivity and  $MB_{jt}$  can change over time and by region. We use the observed  $MB_{jt}$  in case less solar is allocated to a TSO than in the benchmark (observed) case, but allow for lower marginal costs and different marginal emissions - in line with the observed supply curves - in case more solar gets allocated to any given region. Finally, while in the residential reallocation exercise we defined  $\gamma$  as the share of total residential buildings that can be covered with solar panels, this classification no longer applies when using all

<sup>40</sup>ENTSO-E provides high-frequency data at the plant level for conventional power plants. However, these data are available only for large plants with an installed capacity greater than 100 MW.

solar, including large ground-mounted installations. Therefore, we define  $\gamma$  as the share of total generation capacity that is covered by solar in each TSO. In our data, this value ranges from 14% in Amprion to 31% in TenneT South in 2016. We focus on the case of an SCC value of 31.71 €/ tCO<sub>2</sub>, no co-pollutants, and optimal reallocation using the TSO ranking algorithm.

To determine the implied transmission capacities, we follow [Joskow and Tirole \[2005\]](#) and [LaRiviere and Lyu \[2022\]](#) and estimate the following regressions for the marginal costs  $\lambda_{\mathcal{N},t}$  and  $\lambda_{\mathcal{S},t}$  in each region (see the Online Appendix C for their derivation),

$$\begin{aligned} E[\lambda_{\mathcal{N},t}] &= a_{\mathcal{N}} + b_{\mathcal{N}}(S_{\mathcal{N},t} - Q_{\mathcal{N},t}) + c_{\mathcal{N}}Q_{\mathcal{S},t} + FE_{\mathcal{N}} \\ E[\lambda_{\mathcal{S},t}] &= a_{\mathcal{S}} + b_{\mathcal{S}}(S_{\mathcal{S},t} - Q_{\mathcal{S},t}) + c_{\mathcal{S}}Q_{\mathcal{N},t} + FE_{\mathcal{S}} \end{aligned}$$

only using time intervals for which the transmission constraint is binding:  $\lambda_{\mathcal{N},t} \neq \lambda_{\mathcal{S},t}$ .  $Q_{j,t}$  is load in region  $j \in \{\mathcal{N}, \mathcal{S}\}$  at time  $t$  and therefore,  $S_{j,t} - Q_{j,t}$  is the negative of the residual load.  $FEs$  represent year-month-hour and day fixed-effects.

By using only the hours for which the two marginal costs are different in each region we guarantee that the transmission constraint is binding. Therefore, any increases in load in  $\mathcal{N}$  should not affect the scheduling of sources in  $\mathcal{S}$  and viceversa during those hours. This exogenous covariate serves as a valid supply shifter in the estimation of an otherwise endogenous regression. [Table 2](#) shows the results. The expressions above are supply functions since as the size of the capacity constraint  $K$  increases, exports increase and more expensive technologies need to be used: higher  $\lambda_j$ . Our regressions use the spread in the marginal costs of electricity across the two regions as evidence of congestion similarly to [Fell et al. \[2020\]](#). However, we use this spread to define the eligible set of observations to include in our regressions, as opposed to including a function of the spread as a regressor.<sup>41</sup>

Based on the results in the Online Appendix C, we find that

$$\text{capacity imbalance}_t = \Delta K_t = \frac{\Delta z_t}{b_{\mathcal{N}} - b_{\mathcal{S}}}, \quad (2)$$

---

<sup>41</sup>Online Appendix Table D.3 shows the results when we allow for the possibility that load in the other TSOs might impact our estimates for TenneT. The main coefficients are not statistically different from each other (critical z-values of -0.94 and -0.02 in Columns (1) and (2), respectively). Calculating the implied transmission capacity based on these estimates yields a comparable mean of 3,763 MW.

Table 2: Estimates of Shadow Costs of Transmission

	(1)	(2)	(3)	(4)	(5)	(6)
	Gap > 2 €/ MWh		Gap > 5 €/ MWh		Gap > 8 €/ MWh	
	$\lambda_{\mathcal{N}}$	$\lambda_{\mathcal{S}}$	$\lambda_{\mathcal{N}}$	$\lambda_{\mathcal{S}}$	$\lambda_{\mathcal{N}}$	$\lambda_{\mathcal{S}}$
$S_{\mathcal{N}} - Q_{\mathcal{N}}$	-0.000932** (0.000301)		-0.000984** (0.000298)		-0.000480 (0.000418)	
$Q_{\mathcal{S}}$		-0.00118 (0.000820)		-0.00127 (0.000814)		-0.00128 (0.00101)
$S_{\mathcal{S}} - Q_{\mathcal{S}}$		-0.00634*** (0.000586)		-0.00653*** (0.000606)		-0.00730*** (0.000675)
$Q_{\mathcal{N}}$		0.00196* (0.000878)		0.00217* (0.000889)		0.00329** (0.00102)
Constant	13.35** (4.645)	-23.02* (8.991)	13.42** (4.660)	-26.24** (9.086)	19.13*** (5.424)	-41.72*** (10.71)
$N$	4,461	4,461	4,398	4,398	3,787	3,787
$R^2$	0.820	0.708	0.823	0.711	0.834	0.708

*Notes:* Dependent variable: as indicated on top of each column. “Gap” is the absolute value of the difference between the two marginal costs. Standard errors clustered at the date level. \*  $p < 0.05$ , \*\*  $p < 0.01$ , \*\*\*  $p < 0.001$ .

where  $z_t \equiv \lambda_{\mathcal{N},t} - \lambda_{\mathcal{S},t}$  and  $\Delta z_t = z_t - z_{t-1}$ . Let  $\overline{\Delta K}$  be the mean of the distribution of  $\Delta K_t$ . Then, the imputed marginal cost in region  $\mathcal{N}$  can be written as

$$\lambda_{\mathcal{N},t} = \lambda_{\mathcal{S},t} + z_{t-1} + (b_{\mathcal{N}} - b_{\mathcal{S}})\overline{\Delta K}. \quad (3)$$

Figure D.6 in the Online Appendix shows the implied transmission capacities for each of our feasible data points as a function of the solar output in the South region using Equation 2. The mean of these values is 3,487 MW, which is roughly equivalent to twice the capacity of the TenneT transmission line to Norway or about four times the capacity of a new projected interconnection to the Netherlands.<sup>42</sup> Similarly, the SuedOstlink project between TenneT and 50Hertz is designed for a capacity of 2,000 MW with possibility of an expansion to 4,000 MW.<sup>43</sup> Those projects indicate that our estimates are well within reasonable values in the industry for this market.

With Equation 3 in hand, we can re-do the reallocation simulation for different values of the transmission capacity that replace the value of  $\overline{\Delta K}$  in that same equation. For low values of this capacity, the marginal cost differential  $z_t$  is similar in value to the marginal cost in

<sup>42</sup>Tennet [2020b].

<sup>43</sup>50 Hertz [2020].

the previous period. Therefore, we expect that for capacities close to 0, the misallocation of solar will remain similar to the case of no increase in transmission capacity.

If production in the South is higher than total load in that region, the excess amount is then exported to the North whenever this amount is less or equal than the size of the added transmission capacity. This quantity is valued at the corresponding marginal benefit in the North at that given point in time. Given our transmission model, we focus on the additional benefits from displaced production costs and abstract from additional effects on emissions in the North region, as highlighted by [Fell et al. \[2020\]](#).<sup>44</sup> In the absence of the new transmission capacity, the surpluses in the South would be valued at 0. Since this transmission line can carry electricity from any source, and is particularly relevant for large RES plants, we use the total amount of solar capacity installed in Germany in 2016 to conduct our reallocation counterfactuals. In addition, given that most observations fall within a range of 6,000 MW in Online Appendix Figure D.6 and the projected line capacities in the NDP, we limit the amount of additional transmission capacity to be no more than 6,000 MW.

[Figure 7](#) shows the gains from reallocating solar as a function of  $\gamma$  for different values of the capacity constraint  $\Delta K$ . We find that the gains from reallocating solar capacity are larger than without this additional transmission capacity.<sup>45</sup> For relatively low levels of  $\gamma$  the gains are increasing as in the case without transmission, i.e. when optimizing the solar allocation total gains increase as long as the capacity constraint in the TSO is not binding (solar production<sub>*j*</sub>  $\leq$  load<sub>*j*</sub>).

Once solar output is placed in high-productivity regions, particularly in South TenneT, the excess can be exported to the North region provided there is sufficient transmission capacity available. If there is no additional capacity in transmission ( $\Delta K = 0$ ), the surplus in solar output from the South cannot displace further conventional plants and the gains decrease because the reallocation takes solar capacity from other regions that could have utilized it. As  $\Delta K$  increases, the gains become considerably larger, i.e. a capacity constraint

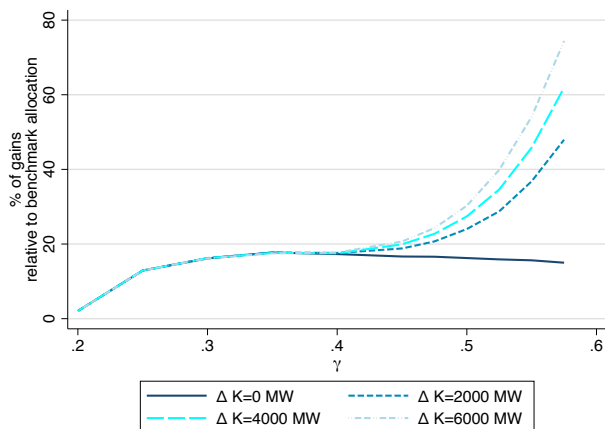
---

<sup>44</sup>Since we simulate the marginal cost for the North region as a function of  $\Delta K$ , there is not a direct mapping from marginal costs to emissions.

<sup>45</sup>Note that the minimum  $\gamma$  is set at 0.2, which results in approximately zero gains from reallocation. We allow  $\gamma$  to increase up to 58% of each TSO's capacity.

of 2,000 MW evaluated at  $\gamma = 0.55$  leads to approximately double the gains compared to the case without interconnection. The increasing gains, reflect the fact that the excess of solar production in the South valued at its corresponding marginal benefits value in the North more than offsets the losses in benefits in the regions where solar capacity has been decreased. Online Appendix Figure D.7 shows the allocation shares with and without interconnection capacity  $\Delta K$ , and highlights that at high levels of  $\gamma$ , more capacity will be allocated to TenneT South in case capacity is available, as the gains in this region are larger.

Figure 7: Gains from Expanding Transmission Capacity



*Notes:* Each curve depicts the gains from reallocation if the transmission capacity between regions North and South is expanded by the amount indicated in the legend. We show the allocation for the example of  $\Delta K \in \{0, 2000 \text{ MW}\}$  in Online Appendix Figure D.7.

We now turn to a back-of-the-envelope calculation to compare the costs and benefits of a new transmission line using our misallocation estimates. We report different scenarios in Table 3. In line with the above findings, the table shows that additional gains from reallocation for relatively low levels of  $\gamma$  are small. As  $\gamma$  increases, the interconnection capacity becomes more valuable. The additional benefits from a capacity expansion of  $\Delta K = 2,000$  MW and with a solar installation rate of  $\gamma = 0.5$  are 386.71 million euros relative to the case where there was no interconnection between the regions but at the same installation rate. We do not take into account the installation costs of the PV plants that would need to be subtracted from those gains. The main reason is that we do not have information on how

many years are left in the lifespan of each panel. As a consequence, the benefits-costs ratios below are biased upwards.

We compare those gains to the tentative investment cost of the underground transmission lines that are currently under construction in Germany (SuedOstlink) with that same capacity (2,000 MW) and a total length of 580 km. This cost is estimated to be approximately 5 billion euros, which has an annualized value of approximately 151 million euros when using a lifetime of 40 years in line with the official amortization period of this project, and an annual discount rate of 1% as in [Davis and Hausman \[2016\]](#).

For the realized underground cables, the benefit-cost (BC) ratios are greater than one only in the case where we consider large values of  $\gamma$ . At 30%, close to the observed solar-to-capacity share in TenneT South, we show that investment is not beneficial. On the other hand, once we allow for larger reallocation values of 50%, the BC ratios are positive (2.56 and 2.31, depending on the size of the transmission line).<sup>46</sup> Not surprisingly, the project would lead to larger benefits if traditional overhead lines were used that are considered to be 10 to 15 times cheaper as underground cables.<sup>47</sup> The BC analysis shows that additional transmission can be beneficial if there is sufficient RES capacity reallocated across regions. This is especially important if we were to consider different types of RES technologies that are more abundant in different regions, as it is the case for wind and solar in the North and South of Germany.

## 6 Conclusion

We develop a comprehensive framework to measure misallocation of RES, and in particular of solar PV plants. This is inspired by the existing rigidity of incentives used to accelerate the adoption of RES. In this paper we concentrated on the uniform nature of feed-in-tariffs. Our framework consists of three steps: measuring the marginal benefits from an additional unit of output from solar, using those valuations to measure the potential gains had an efficient

---

<sup>46</sup>To calculate the expected cost for the 4,000 MW interconnection with underground cables, we rely on cost estimates per km from *Suedlink*, a similar project with 4,000 MW capacity. We find a total investment cost of 7.9 billion euros.

<sup>47</sup>See [Xcel Energy \[2021\]](#). We assume a cost factor of 8%, the midpoint between the two cost estimates.

Table 3: Benefit-Cost Analysis for Power Line Investment

Planned interconnection, $\Delta K$ [MW]	2,000			4,000		
<b>Annualized investment costs</b> [m€]						
Overhead lines	12.06			19.93		
Underground lines	150.77			249.14		
Capacity share, $\gamma$	0.3	0.4	0.5	0.3	0.4	0.5
<b>Annual gains from reallocation</b> [m€]	5.11	14.81	386.71	3.47	10.39	554.69
<b>Benefit-cost ratio</b>						
Overhead lines	0.42	1.23	32.06	0.18	0.54	28.94
Underground lines	0.03	0.10	2.56	0.01	0.04	2.31

*Notes:* Change in gains from reallocation for given  $\gamma$  comparing the case of no interconnection with interconnection scenarios of 2,000 and 4,000 MW, respectively. Annualized investment costs for underground lines based on *SuedOstLink* project, with estimated total costs of 5 billion (bn) euros (Source: TenneT). For the 4,000 MW transmission, we assume a total cost of 7.94bn euros, using the cost per kilometer from the alternative *Suedlink* project, a transmission line with 4,000 MW capacity. For overhead lines we assume that total investment cost represents approximately 8% of the underground cables. For both type of high-voltage lines we consider furthermore a 40 year lifespan and a 1% annual discount rate.

allocation of solar PV installations existed, and accounting for further gains if expansions in transmission capacities are built.

We apply our framework to the case of Germany and we find evidence of heterogeneous marginal benefits from increasing the solar capacity even when using a conservative value of the social cost of carbon. We find economically relevant gains relative to the current allocation if solar panels had been allocated according to their solar productivity and marginal benefits. In addition, if a new transmission line were built between the North and the South regions, this would increase the gains from reallocating solar PV plants for medium-high levels of the feasible solar penetration rate.

As any economics analysis, ours does not go without caveats. We focused on solar installations but a more comprehensive study would include wind installations as well. In the best case scenario, there is no misallocation of wind plants in Germany and the total gains from misallocation would only be caused by misalignments in incentives for solar plants. Therefore, we can see our results as a lower bound on the gains from potential misallocation. Another avenue for future research is to include transmission constraints across the different regions to be able to value surpluses if they exist. Once again, our results can be seen as a lower bound for the true gains since we are implicitly valuing excess solar production, if

any, at a marginal benefit of zero. In either of those two cases our framework can be easily extended if more data were available.

The efficiency of the allocation of resources is a core paradigm in economics. Our paper quantifies this efficiency and puts in perspective the costs of simple economic incentives for technology adoption.

## References

- 50 Hertz (2020). Onshore Projects SuedOstLink. <https://www.50hertz.com/en/Grid/Griddevelopment/Onshoreprojects/SuedOstLink>. Last accessed September 7, 2020.
- Abrell, J., Kosch, M., and Rausch, S. (2019a). Carbon Abatement with Renewables: Evaluating Wind and Solar Subsidies in Germany and Spain. *Journal of Public Economics*, 169:172–202.
- Abrell, J., Rausch, S., and Streitberger, C. (2019b). The Economics of Renewable Energy Support. *Journal of Public Economics*, 176:94–117.
- Ambec, S. and Crampes, C. (2019). Decarbonizing Electricity Generation with Intermittent Sources of Energy. *Journal of the Association of Environmental and Resource Economists*, 6(6):1105–1134.
- Asker, J., Collard-Wexler, A., and De Loecker, J. (2019). (Mis) allocation, Market power, and Global Oil Extraction. *American Economic Review*, 109(4):1568–1615.
- Bahn, O., Samano, M., and Sarkis, P. (2020). Market Power and Renewables: The Effects of Ownership Transfers. *Energy Journal*.
- Baker, E., Fowlie, M., Lemoine, D., and Reynolds, S. S. (2013). The Economics of Solar Electricity. *Annu. Rev. Resour. Econ.*, 5(1):387–426.
- Borenstein, S. (2012). The Private and Public Economics of Renewable Electricity Generation. *The Journal of Economic Perspectives*, 26(1):67–92.
- Borenstein, S. and Bushnell, J. B. (2022). Do Two Electricity Pricing Wrongs Make a Right?

- Cost Recovery, Externalities, and Efficiency. *American Economic Journal: Economic Policy*.
- Callaway, D. S., Fowle, M., and McCormick, G. (2018). Location, Location, Location: The Variable Value of Renewable Energy and Demand-side Efficiency Resources. *Journal of the Association of Environmental and Resource Economists*, 5(1):39–75.
- Carvallo, J. P., Zhang, N., Murphy, S. P., Leibowicz, B. D., and Larsen, P. H. (2020). The Economic Value of a Centralized Approach to Distributed Resource Investment and Operation. *Applied Energy*, 269:115071.
- Cullen, J. (2013). Measuring the Environmental Benefits of Wind-generated Electricity. *American Economic Journal: Economic Policy*, 5(4):107–33.
- Davis, L. and Hausman, C. (2016). Market Impacts of a Nuclear Power Plant Closure. *American Economic Journal: Applied Economics*, 8(2):92–122.
- Durrmeyer, I. and Samano, M. (2018). To Rebate or Not to Rebate: Fuel Economy Standards versus Feebates. *The Economic Journal*, 128(616):3076–3116.
- ENTSO-E (2018). TYNDP (Network Development Plan). <https://tyndp.entsoe.eu/tyndp2018>. Last accessed June 9, 2020.
- EPA (2016). Social Cost of Carbon Fact Sheet. [https://www.epa.gov/sites/production/files/2016-12/documents/social\\_cost\\_of\\_carbon\\_fact\\_sheet.pdf](https://www.epa.gov/sites/production/files/2016-12/documents/social_cost_of_carbon_fact_sheet.pdf). Last accessed June 9, 2020.
- Fabra, N. and Montero, J. P. (2022). Technology-Neutral vs. Technology-Specific Procurement. *The Economic Journal*. Forthcoming.
- Federal Ministry for Economic Affairs and Energy (BMWi) (2015). An Electricity Market for Germany’s Energy Transition. [https://www.bmwi.de/Redaktion/EN/Publikationen/whitepaper-electricity-market.pdf?\\_\\_blob=publicationFile&v=7](https://www.bmwi.de/Redaktion/EN/Publikationen/whitepaper-electricity-market.pdf?__blob=publicationFile&v=7). Last accessed July 7, 2021.
- Fell, H., Kaffine, D. T., and Novan, K. (2020). Emissions, Transmission, and the Environ-

- mental Value of Renewable Energy. *American Economic Journal: Policy*.
- Fell, H. and Linn, J. (2013). Renewable Electricity Policies, Heterogeneity, and Cost Effectiveness. *Journal of Environmental Economics and Management*, 66(3):688–707.
- Fowlie, M. and Muller, N. (2019). Market-based Emissions Regulation when Damages vary across Sources: What are the Gains from Differentiation? *Journal of the Association of Environmental and Resource Economists*, 6(3):593–632.
- Fowlie, M., Reguant, M., and Ryan, S. P. (2016). Market-based Emissions Regulation and Industry Dynamics. *Journal of Political Economy*, 124(1):249–302.
- Furtwängler, C. and Weber, C. (2019). Spot and Reserve Market Equilibria and the Influence of New Reserve Market Participants. *Energy Economics*, 81:408–421.
- Gerster, A. and Lamp, S. (2020). Energy Tax Exemptions and Industrial Production. *Working Paper*.
- Gillingham, K. and Ovaere, M. (2020). The Heterogeneous Value of Solar and Wind Energy: Empirical Evidence from the United States and Europe. Working Paper.
- Gowrisankaran, G., Reynolds, S. S., and Samano, M. (2016). Intermittency and the Value of Renewable Energy. *Journal of Political Economy*, 124(4):1187–1234.
- Green, R., Staffell, I., and Vasilakos, N. (2011). Divide and Conquer? Assessing k-means Clustering of Demand Data in Simulations of the British Electricity System. Technical report, Available from <http://tinyurl.com/c934prp>.
- Hirth, L. (2015). Balancing Power. <https://neon-energie.de/balancing-2015.pdf>. Last accessed June 12, 2019.
- Holland, S. P., Mansur, E. T., Muller, N. Z., and Yates, A. J. (2016). Are there Environmental Benefits from Driving Electric Vehicles? The Importance of Local Factors. *American Economic Review*, 106(12):3700–3729.
- Jarvis, S., Deschenes, O., and Jha, A. (2022). The Private and External Costs of Germany’s Nuclear Phase-Out. Technical report.

- Joskow, P. and Tirole, J. (2005). Merchant Transmission Investment. *The Journal of Industrial Economics*, 53(2):233–264.
- Knittel, C. R., Metaxoglou, K., and Trindade, A. (2016). Are we Fracked? The Impact of Falling Gas Prices and the Implications for Coal-to-gas Switching and Carbon Emissions. Technical report.
- LaRiviere, J. and Lyu, X. (2022). Transmission Constraints, Intermittent Renewables and Welfare. *Journal of Environmental Economics and Management*.
- Leslie, G. (2018). Tax Induced Emissions? Estimating Short-run Emission Impacts from Carbon Taxation under Different Market Structures. *Journal of Public Economics*, 167:220–239.
- Ministry of Economy and Energy (2000). Renewable Energy Act (EEG). [https://www.erneuerbare-energien.de/EE/Redaktion/DE/Dossier/eeg.html?cms\\_docId=71110](https://www.erneuerbare-energien.de/EE/Redaktion/DE/Dossier/eeg.html?cms_docId=71110). Last accessed June 9, 2020.
- Neon Neue Energieökonomik, Technical University of Berlin, DIW Berlin, and ETH Zürich (2019). Open Power System Data. <https://open-power-system-data.org>. Last accessed February 7, 2022.
- Network Development Plan (2019). Network Development Plan 2030. <https://www.netzentwicklungsplan.de/de/projekte/projekte-nep-2030-2019>. Last accessed February 7, 2022.
- Netztransparenz (2018). EEG Anlagenstammdaten. <https://www.netztransparenz.de/EEG/Anlagenstammdaten>. Last accessed June 9, 2020.
- Next Kraftwerke (2020). Regelenergie. <https://www.next-kraftwerke.de/wissen/regelenergie>. Last accessed June 9, 2020.
- Novan, K. (2015). Valuing the Wind: Renewable Energy Policies and Air Pollution Avoided. *American Economic Journal: Economic Policy*, 7(3):291–326.
- Philipps, S. and Warmuth, W. (2018). Photovoltaics Report. <https://www.ise>.

- [fraunhofer.de/en/publications/studies/photovoltaics-report.html](https://www.fraunhofer.de/en/publications/studies/photovoltaics-report.html). Fraunhofer ISE and PSE Projects GmbH. Last accessed September 23, 2021.
- Pollitt, M. G. and Anaya, K. L. (2020). Competition in Markets for Ancillary Services? The Implications of Rising Distributed Generation. *The Energy Journal*, 41(Special Issue).
- PV Output (2020). PV Output Data. <https://pvoutput.org>. Last accessed June 9, 2020.
- Regelleistung (2018). Data for Control Reserve. <http://regelleistung.net>. Last accessed June 9, 2020.
- Regelleistung (2020). ReBAP Model. [https://www.regelleistung.net/ext/download/REBAP\\_MODELL\\_20200701](https://www.regelleistung.net/ext/download/REBAP_MODELL_20200701). Last accessed June 9, 2020.
- Reguant, M. (2019). The Efficiency and Sectoral Distributional Impacts of Large-scale Renewable Energy Policies. *Journal of the Association of Environmental and Resource Economists*, 6(S1):S129–S168.
- Sexton, S., Kirkpatrick, A. J., Harris, R. I., and Muller, N. Z. (2021). Heterogeneous Solar Capacity Benefits, Appropriability, and the Costs of Suboptimal Siting. *Journal of the Association of Environmental and Resource Economists*, 8(6):1209–1244.
- Sinn, H.-W. (2017). Buffering Volatility: A Study on the Limits of Germany’s Energy Revolution. *European Economic Review*, 99:130–150.
- Stiglitz, J. E. (2019). Addressing Climate Change Through Price and Non-price Interventions. *European Economic Review*, 119:594–612.
- Tangeras, T. and Wolak, F. (2019). Optimal Network Tariffs for Renewable Electricity Generation. Working paper.
- Tennet (2020a). Direct Current Connections SuedLink and SuedOstLink. <https://www.tennet.eu/de/news/news/gleichstromverbindungen-suedlink-und-suedostlink-netzbetreiber-starten-ausschreibungen-fuer-erdkabel> Last accessed September 7, 2020.
- Tennet (2020b). International Connections Nordlink. <https://www.tennet.eu/our-grid/>

[international-connections/nordlink/](#). Last accessed September 7, 2020.

Timera Energy (2014). German Recession, Power Prices & Generation Margins. <https://timera-energy.com/german-recession-power-prices-generation-margins>. Last accessed June 12, 2019.

Wibulpolprasert, W. (2016). Optimal Environmental Policies and Renewable Energy Investment: Evidence from the Texas Electricity Market. *Climate Change Economics*, 7(04):1650010.

Wolak, F. A. (2015). Measuring the Competitiveness Benefits of a Transmission Investment Policy: The Case of the Alberta Electricity Market. *Energy Policy*, 85:426–444.

Xcel Energy (2021). Overhead vs Underground. [https://www.xcelenergy.com/staticfiles/xcel/Corporate/Corporate%20PDFs/OverheadVsUnderground\\_FactSheet.pdf](https://www.xcelenergy.com/staticfiles/xcel/Corporate/Corporate%20PDFs/OverheadVsUnderground_FactSheet.pdf). Last accessed September 10, 2021.

Zerrahn, A., Schill, W.-P., and Kemfert, C. (2018). On the Economics of Electrical Storage for Variable Renewable Energy Sources. *European Economic Review*, 108:259–279.

# Online Appendix for “(Mis)allocation of Renewable Energy Sources”

Stefan Lamp\*      Mario Samano<sup>†</sup>

November 3, 2022

## A Details on Data and Simulation Procedure

### A.1 Simulated frequencies of marginal technologies

#### Independent TSOs

In the main section of the paper, we consider the case in which each TSO balances supply and demand independently. While in 2015 and 2016 there exists a unique price zone for the entire German - Austrian market, we refrain from using wholesale market prices in our analysis and model supply in each of the TSOs independently. This approach allows us to take into account differences in the production-mix across TSOs when measuring the marginal benefits of solar. This modeling choice is supported by increasing congestion and lack-of-balancing concerns that led to the disintegration of the Germany-Austria bidding zone in 2018.<sup>1</sup> We perform further robustness checks concerning the use of a single market as explained in the “Single Market” subsection below.

To obtain the simulated frequencies presented in [Table A.1](#), we rely on fuel price data to establish a ranking of the different technologies. While there is a world market price for hard coal, crude oil, and natural gas, this is usually not the case for brown coal (lignite) and uranium (nuclear energy). Therefore, we rely on energy market modelling data from [ENTSO-E \[2018\]](#) for these type of fuels, and complement this information with emission factors for lignite in Germany from the [German Environmental Ministry \[2017\]](#). From there,

---

\*Universidad Carlos III Madrid. Email: [slamp@eco.uc3m.es](mailto:slamp@eco.uc3m.es)

<sup>†</sup>HEC Montreal. Email: [mario.samano@hec.ca](mailto:mario.samano@hec.ca)

<sup>1</sup>While there exists no publicly available data on congestion for the entire German electricity grid, 50Hertz publishes hourly congestion data. These data are available in a binary format from [Staudt et al. \[2019\]](#) for the years 2015 to 2017, indicating that about 3% of the lines are congested at all hours, when defining congestion according to the 50% thermal capacity threshold. According to KIT, most grid congestion (96%) appears in the two largest TSOs, 50Hertz and TenneT. Congestion and increasing balancing needs also contributed to the planning and construction of new high-voltage power lines (Suedlink, Sued-Ost Link) as discussed in the paper.

we obtain that the simulated merit-order supply curve has the following order, listed from cheapest to most expensive source: 1) renewables (wind onshore and offshore, solar, hydro (reservoir, run of river, pumped storage), geothermal, and other renewables), 2) nuclear, 3) biomass and waste, 4) lignite, 5) hard coal, 6) gas, and 7) oil. In the specific case of 50Hertz we furthermore make the assumption that oil is always infra-marginal, as electricity production from ‘oil’ is linked to an oil refinery (IKS Schwedt) that produces electricity as a by-product in its main production process. We verify this information in our data by plotting the electricity production profile for this plant, which shows no variation over time.

Table A.1: Simulated Frequencies of Marginal Technologies

Source	Freq.	Percent
Natural Gas	172,501	61.45
Hard Coal	100,765	35.90
Nuclear	3,522	1.25
Oil	3,187	1.14
Brown Coal / Lignite	655	0.23
Hydro: River	46	0.02
Hydro: Pumped storage	24	0.01
Biomass	4	0.00

*Notes:* For each 15-minute interval of the day we compute the marginal cost of each of the technologies shown in the table, we sort them from lowest to highest marginal cost to obtain the system’s marginal cost curve. Notice that the marginal cost for fossil fuels can change over time as we use fuel prices data to construct this curve. Finally, we select the technology that corresponds to the point in the marginal cost curve that intersects the net load in that time interval.

## Single Market

We provide robustness checks for our main findings by treating Germany as a single market. To determine the marginal technology in this case, we follow a similar approach as above but aggregating all the sources Germany-wide. As for most time intervals there is positive production for most of the technologies, we follow an approach similar to [Germeshausen and Wölfing \[2020\]](#). To determine the price-setting technology in the German market, we use data from [Consentec GmbH \[2016\]](#) to document the minimum (must-run) requirements for each of the technologies. Following this approach, we obtain the following frequencies of marginal technologies, which are largely comparable to the frequencies found in the TSO-specific dispatch case ([Table A.1](#)).

## CO<sub>2</sub> prices

In our analysis, we abstract from the CO<sub>2</sub> prices from the European Union Emission Trading Scheme (EU-ETS). While electricity production in Europe is subject to the EU-ETS, CO<sub>2</sub>

Table A.2: Simulated Frequencies of Marginal Technologies, single market

Source	Freq.	Percent
Natural Gas	49,988	71.23
Hard Coal	14,187	20.22
Oil	2,912	4.15
Brown Coal / Lignite	2,592	3.69
Nuclear	465	0.66
Biomass	32	0.05

*Notes:* For each 15-minute interval of the day we compute the marginal cost of each of the technologies shown in the table, we sort them from lowest to highest marginal cost to obtain the system’s marginal cost curve for the entire market in Germany, pooling all TSOs. The marginal-cost ordering takes into account “must-run” capacities as in [Consentec GmbH \[2016\]](#) that operate independently of prices.

prices during the time of our analysis (2015-16) have been at an all-time low. This was likely due to oversupply of emission certificates. In 2015, the average price per tCO<sub>2</sub> was less than 10 €. In 2016, the price decreased further to approximately 5 €/ tCO<sub>2</sub>. Given the price differentials in marginal costs in electricity production (fuel input prices), the low CO<sub>2</sub> prices should not have led to changes in the aggregate merit-order cost curve (see for instance [Energy Brain Pool \[2017\]](#)). We therefore refrain from modeling variations in CO<sub>2</sub> prices.

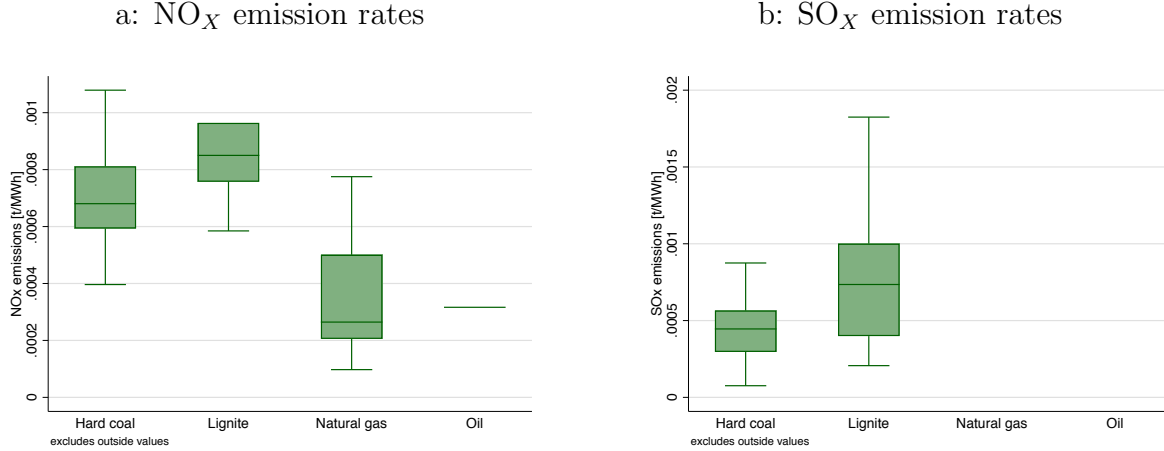
## A.2 Co-pollutants

We obtain plant-level production data from individual fossil-fuel power plants in Germany (ENTSO-E) and combine them with data on co-pollutants published for large combustion plants from the European Pollutant Release and Transfer Register (E-PRTR). As these datasets do not share a common identifier, we match them manually using plant name, fuel type, and location. To do so, we first match the electricity production data to the list of individual power plants, available from OPSD [[Neon Neue Energieökonomik et al., 2019](#)], which provides further covariates that facilitates matching with the pollution data. We are able to match more than 80% of power plants for these datasets uniquely. As the pollution registry is only available at the firm-location level, we aggregate individual electricity production plants at the firm level in case they share the same location and type of fuel. We are again able to match approximately 80% of the pollution data for thermal power stations to the list of power plants. Yet, the sample of firms that report pollution and production data does not fully overlap. Our final dataset is comprised of 46 unique firms for nitrogen oxides (NO<sub>x</sub>) pollution and 33 firms for sulfur oxides (SO<sub>x</sub>) pollution that we observe over our sample period 2015 to 2016.

While NO<sub>x</sub> arises from all fossil fuel combustion types, SO<sub>x</sub> emissions are mostly related to the combustion of hard coal and lignite. We focus our analysis on SO<sub>x</sub> and NO<sub>x</sub> pollution, as these data are widely reported in the E-PRTR, while other pollutants are only reported

for a small selection of firms. Moreover, the fact that our main level of analysis is at the TSO level, we believe that both these co-pollutants play an important role in determining health outcomes, while other pollutants might only have highly localized effects, such as particulate matter.

Figure A.1: Co-pollutants: emission rates (t/MWh)



*Notes:* Box plots show the distribution of emission rates (t/MWh) by technology (type of fuel). Outside values have been removed for ease of exposition.

To quantify the impact of co-pollutants, we use the median emission rate as shown in Figure A.1 for each of the technologies and multiply each ton of pollutant by the following values of damages: for NO<sub>x</sub> we use 2,021.79 €/ ton and for SO<sub>2</sub> we use 34,051.2 €/ ton, which are based on Holland et al. [2005].<sup>2</sup> We account for co-pollutants the same way as was done for CO<sub>2</sub> emissions in our marginal benefits calculation.

### A.3 Reallocating RES

For the reallocation exercise in Section 5.1 of the paper, we take the total residential solar capacity on the last day of our sample (31 December 2016) as given. Similarly, we obtain data for total installed capacity (all generating units) per TSO. We calculate the total residential solar output per time interval, using total solar output by TSO and multiplying it by the fraction of residential to total solar capacity. We complement these data by using individual solar PV production data, obtained from PV Output [2020]. These data allow us to account for heterogeneity in residential solar output within each TSO. We calculate the baseline value (marginal costs + marginal emissions + change in ancillary service costs) of actual solar PV production using these data. In a next step, we use the algorithm described in the main text to reallocate solar capacity given a range of FSPRs ( $\gamma$  values).

<sup>2</sup>More specifically, we multiplied the numbers from Holland et al. [2005] in Tables 9 and 11, last column, by an inflation factor to convert the 2010 euro estimates from those tables into constant 2015 euros (the factor is 1.0641).

## A.4 The value of transmission

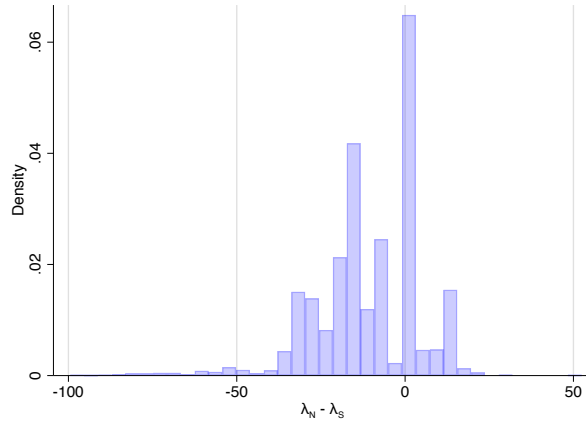
We construct simulated supply curves for both North and South TenneT following the approach described in Section 5.3 in the paper, using the following capacity factors for conventional power plants obtained from EIA [2020]: geothermal: 0.72; hydro: 0.37; nuclear: 0.92; biomass & waste: 0.63; hard coal & lignite: 0.53; natural gas: 0.55; oil: 0.13; and other fuels: 0.5. For wind (offshore and onshore) as well as solar, we can rely on observed production data as these technologies are always inframarginal. In a next step, we obtain high frequency data on plant outages and planned shutdowns for maintenance from ENTSO-E and combine these data with total installed capacity. We take total installed capacity of conventional power plants by TSO at the beginning of 2015. This modeling choice is especially relevant for the production capacities in Bavaria, where a large nuclear plant has been shut down during 2015 and has been replaced by increasing imports through the Austria and Czech interconnections. As we do not model imports/exports to neighboring countries, this assumption guarantees that there is sufficient installed capacity in Bavaria to meet demand. We furthermore obtain detailed (15-min) data on total solar PV production in Bavaria, available from TenneT, which allow us to have realized solar production data for both the North and South regions.

Based on these data, we construct an aggregate supply curve by TSO that we intersect with aggregate load. We split load for North and South TenneT based on its population share. These data allow us to construct the marginal costs ( $\lambda_{N,t}$  and  $\lambda_{S,t}$ ) as well as marginal emissions, for both regions. We report here how the newly calculated  $\lambda$ 's compare to the main section (Figure 3 and Table 1 in the paper). As North TenneT has more production capacities, we find that the median cost is lower (17.38 €/MWh) compared to the South region (24.24 €/MWh). Nevertheless, the two values are highly comparable to the other TSOs. We plot the differences between  $\lambda_{N,t}$  and  $\lambda_{S,t}$  in Figure A.2. Note that there is a large amount of observations for which the absolute value of this gap is greater than zero, the exact number of those observations at different levels of the gap are as described in Table 2 in Section 5.3 of the paper.

To determine the average capacity utilization of conventional power plants, we use data from the US electricity market (Energy Information Agency) and assign these values to the installed capacity in North and South TenneT. Using data that are external to the German market, allows us to overcome potential endogeneity issues that would stem from using average observed technology shares for the German market. We combine these data with detailed information on plant unavailability for different generation units in TenneT. These data are available from ENTSO-E for 'important' changes in capacity (changes of 100 MW or more in actual availability) for all technologies at high frequency. We then can construct hourly supply curves for conventional power plants  $i$  using the following formula:  $\text{avg. capacity factor}_a \times \sum_i (\text{capacity installed}_i - \text{capacity unavailable}_{it})$ , by type of technology  $a$ . For solar production, which is always inframarginal, we observe the total solar output of all plants in Bavaria at high levels of disaggregation (15-minute) from TenneT. In the construction of the supply curves, we rely on the same marginal cost ordering that we used in Section 4 of the paper.

Regarding demand, we use data on the population shares to split total load in TenneT in

Figure A.2: Differences in Marginal Costs of Electricity Production: North vs. South  
TenneT



*Notes:* Differences of  $\lambda_{N,t}$  and  $\lambda_{S,t}$  based on simulated supply and demand in the two regions.

the two regions. With the aggregate hourly supply and demand curves for each region, we can find their intersection to obtain the marginal technology similarly to our analysis in the previous section. We denote their marginal costs  $\lambda_{N,t}$  for the North and  $\lambda_{S,t}$  for the South regions, respectively and at time  $t$ . We provide additional statistics on the marginal cost estimates for the two regions in TenneT below that show that the split leads to values that are comparable with those in the main part of the paper.

Finally, with these data at hand, we can simulate the reallocation for different values of  $\gamma$  and the transmission constraint  $\Delta K_t$ . As the reallocation is based on *the entire solar capacity*, we rely on aggregate TSO  $\times$  15-minute data, with a total of five TSOs. We use the simulated data on marginal costs and marginal emissions for North and South, as well as observed solar production in the two entities to calculate the baseline value (assuming all TSOs are independent). As before, we recalculate changes in the impact on ancillary service costs, but assume constant gains from marginal costs and marginal emissions. We evaluate solar production in each TSO at its marginal benefit as long as total solar production is smaller or equal to total load. If there is excess production in one region, but no possibility to export, we cap the gains at the load level. Note that this assumption is not as restrictive as it looks at first sight given current levels of grid congestion in Germany. When there is excess production in TenneT South, we allow this region to export energy to the TenneT North region, in line with the transmission capacity  $\Delta K_t$ . This energy surplus is valued at the simulated  $\lambda_{N,t}$ , which is computed following Equation (3) in the paper.

## B Ancillary Services, Load, and Solar Output

We use the  $k$ -means clustering method, which is an unsupervised machine learning algorithm.<sup>3</sup> We define a data point as the vector of all the observed load amounts in one day aggregated at the hourly level and at the TSO level. To this vector we add an additional entry equal to the maximum of those 24 elements to increase the differentiation among the load profiles. The  $k$ -means clustering algorithm starts with  $k$  randomly chosen points and attempts to classify the remaining observations by the proximity to those initial points: each observation gets assigned to the closest of the  $k$  initial points. We use the Euclidian distance in our implementation and several different initial points to make sure our clusters are robust to that initial choice. [Figure B.1](#) shows the mean and standard deviation bands for each of the clusters in each TSO. We determine the number of clusters ( $k = 3$ ) as the maximum value of  $k$  such that the standard deviation bands do not overlap for most of the hours in each TSO.

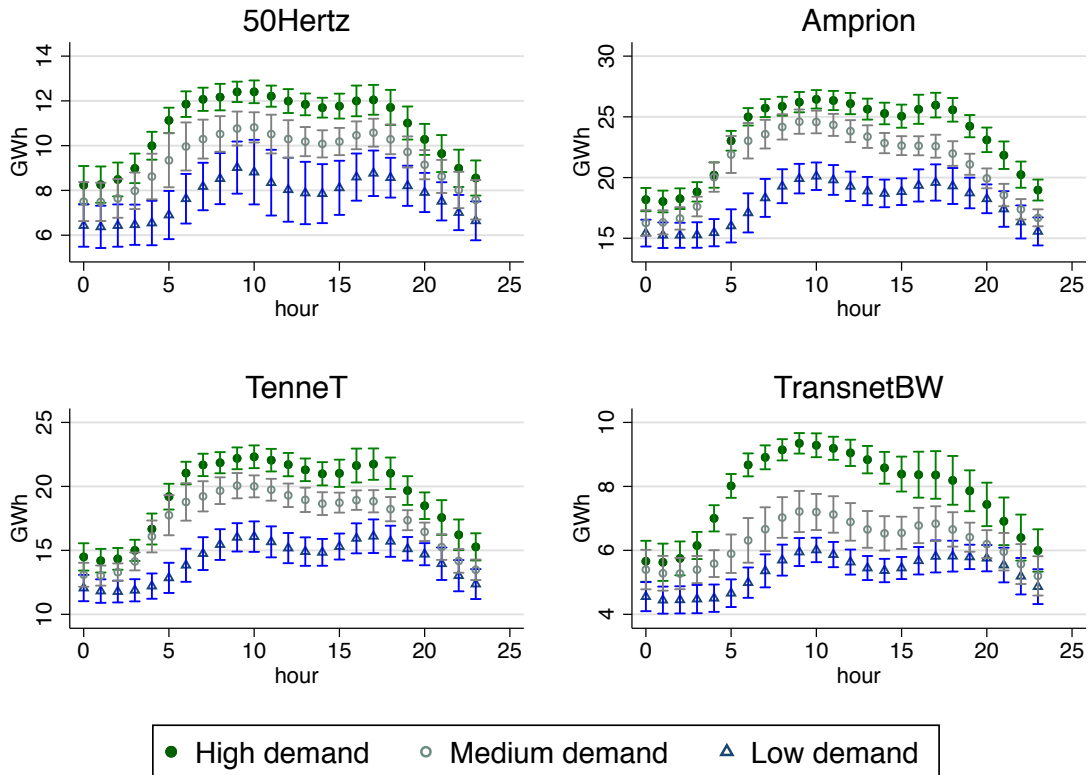
To relate the solar output with the ancillary services costs we cluster the data into categories of load profiles first. We present in [Table B.1](#) and [Table B.4](#) the results from a quadratic and a cubic specifications when pooling all the observations instead of running different regressions by clusters. There, it is evident that by pooling all the observations, there is a loss of heterogeneity of the value of the derivative of interest and fewer coefficients are statistically significant. Therefore, we choose the specification that uses clusters as our main specification.

In order to summarize the regression results, [Table B.5](#) shows the mean of the values of the derivatives of ancillary services costs with respect to solar output when evaluated at each of the time intervals in our sample. [Figure B.2](#) shows plots of these relationships. In the counterfactuals we do not use these averages, but the actual predicted value for costs at each combination of solar output and load as needed.

---

<sup>3</sup>Similarly approaches have been used by [Reguant \[2019\]](#), [Bahn et al. \[2020\]](#), and [Green et al. \[2011\]](#).

Figure B.1: Clusters of Load Profiles by TSO



*Notes:* Each panel shows the mean hourly load profiles grouped into three different clusters and one standard deviation bands for each cluster. Each cluster identifies a different level of demand that we call high, medium, and low. The range of vertical axes is different in each panel to ease readability. The number of clusters ( $k = 3$ ) is the maximum value of  $k$  such that the standard deviation bands do not overlap for most of the hours in each TSO.

Table B.1: Ancillary Costs on Solar and Load by Pooling All Observations

	(1)	(2)
solar	0.174 (0.153)	-0.567 (0.387)
solar <sup>2</sup>	0.0000488*** (0.0000137)	0.000394*** (0.0000682)
load	0.548*** (0.109)	0.723** (0.239)
load <sup>2</sup>	0.00000327 (0.00000300)	-0.00000596 (0.0000165)
solar × load	-0.0000405*** (0.00000792)	-0.0000894* (0.0000402)
solar <sup>3</sup>		-1.49e-08** (4.73e-09)
load <sup>3</sup>		1.07e-10 (3.50e-10)
solar × load <sup>2</sup>		2.86e-09* (1.14e-09)
solar <sup>2</sup> × load		-8.50e-09** (2.81e-09)
FE	✓	✓
<i>N</i>	148,758	148,758
<i>R</i> <sup>2</sup>	0.0411	0.0413

Standard errors in parentheses

\*  $p < 0.05$ , \*\*  $p < 0.01$ , \*\*\*  $p < 0.001$

*Notes:* Dependent variable: ancillary costs. Each regression includes two-way fixed effects of hour of the day, day of the week, month, TSO, and year. Only the coefficients relevant for the derivatives in the main text are reported. In all regressions we use only time observations for which the solar output is positive.

Table B.2: Ancillary Costs on Solar and Load by Cluster of Load Profile (part 1)

	50 Hertz			Amprion		
	(1)	(2)	(3)	(1)	(2)	(3)
solar	5.174 (5.578)	18.44*** (3.778)	6.455 (4.582)	79.60 (108.4)	-20.40 (27.45)	77.84** (27.19)
solar <sup>2</sup>	-0.00223* (0.000933)	-0.00560*** (0.000871)	-0.000391 (0.000839)	0.00101 (0.00526)	-0.000250 (0.00181)	0.00388*** (0.00112)
solar <sup>3</sup>	-9.83e-09 (3.19e-08)	0.000000512*** (7.30e-08)	-3.10e-08 (4.19e-08)	0.000000101 (0.000000108)	0.000000442*** (7.08e-08)	-6.73e-09 (2.96e-08)
load	11.48** (3.595)	8.696** (3.161)	9.625** (3.477)	-237.5*** (71.05)	-4.798 (3.598)	10.94 (25.14)
load <sup>2</sup>	-0.00168*** (0.000429)	-0.00144** (0.000481)	-0.00186*** (0.000462)	0.00906*** (0.00265)	0.000447 (0.000324)	-0.000369 (0.00119)
load <sup>3</sup>	7.20e-08*** (1.60e-08)	7.45e-08** (2.51e-08)	0.000000104*** (1.98e-08)	-0.000000114*** (3.28e-08)	-1.10e-08 (8.59e-09)	4.78e-09 (1.87e-08)
solar × load	0.000380 (0.000791)	-0.00260*** (0.000697)	0.0000577 (0.000616)	-0.00558 (0.00829)	0.00184 (0.00294)	-0.00705** (0.00243)
solar × load <sup>2</sup>	-6.76e-08 (3.49e-08)	0.000000159** (5.04e-08)	-6.62e-08* (2.58e-08)	0.000000103 (0.000000159)	-2.90e-08 (8.02e-08)	0.000000156** (5.47e-08)
solar <sup>2</sup> × load	0.000000189* (7.79e-08)	0.000000185* (9.12e-08)	5.46e-08 (7.31e-08)	-9.49e-08 (0.000000204)	-0.000000117 (8.81e-08)	-0.000000155** (4.99e-08)
<i>N</i>	16,096	7,206	14,426	8,459	10,527	17,649
<i>R</i> <sup>2</sup>	0.108	0.108	0.0850	0.0877	0.0791	0.0790

Standard errors in parentheses

\*  $p < 0.05$ , \*\*  $p < 0.01$ , \*\*\*  $p < 0.001$

*Notes:* Dependent variable: ancillary costs. First three columns correspond to the three clusters of load profiles for 50Hertz and last three columns for Amprion. Each regression includes two-way fixed effects of hour of the day, day of the week, month, and year. Only the coefficients relevant for the derivatives in the main text are reported. In all regressions we use only time observations for which the solar output is positive.

Table B.3: Ancillary Costs on Solar and Load by Cluster of Load Profile (part 2)

	TenneT			TransnetBW		
	(1)	(2)	(3)	(1)	(2)	(3)
solar	380.1*** (40.94)	-3.852 (5.501)	42.15** (13.03)	130.8*** (27.91)	40.25 (31.60)	105.7*** (31.06)
solar <sup>2</sup>	-0.000817 (0.00120)	0.00105** (0.000404)	0.00161*** (0.000451)	0.00561* (0.00240)	0.0160*** (0.00359)	0.0130*** (0.00346)
solar <sup>3</sup>	1.43e-08 (1.87e-08)	-5.31e-09 (1.45e-08)	-1.91e-08* (8.50e-09)	-1.23e-08 (0.000000130)	0.00000132*** (0.000000252)	-0.000000160 (0.000000293)
load	-156.0*** (41.11)	-19.23 (14.47)	-30.01 (19.18)	-129.7*** (25.95)	29.24 (78.57)	-105.6 (79.04)
load <sup>2</sup>	0.00823*** (0.00203)	0.00155 (0.00101)	0.00207 (0.00112)	0.0184*** (0.00320)	-0.00176 (0.0152)	0.0164 (0.0119)
load <sup>3</sup>	-0.000000141*** (3.33e-08)	-3.96e-08 (2.33e-08)	-4.42e-08* (2.19e-08)	-0.000000813*** (0.000000131)	-0.000000129 (0.000000972)	-0.000000827 (0.000000594)
solar × load	-0.0347*** (0.00374)	-0.0000909 (0.000707)	-0.00512*** (0.00143)	-0.0329*** (0.00645)	-0.0217 (0.0121)	-0.0314*** (0.00939)
solar × load <sup>2</sup>	0.000000788*** (8.59e-08)	1.98e-08 (2.44e-08)	0.000000148*** (3.97e-08)	0.00000202*** (0.000000375)	0.00000274* (0.00000118)	0.00000223** (0.000000731)
solar <sup>2</sup> × load	3.51e-08 (5.56e-08)	-5.87e-08* (2.40e-08)	-6.88e-08** (2.44e-08)	-0.000000616* (0.000000274)	-0.00000375*** (0.000000672)	-0.00000150** (0.000000538)
<i>N</i>	10,546	10,575	16,489	23,442	7,474	5,869
<i>R</i> <sup>2</sup>	0.160	0.0624	0.0697	0.0692	0.116	0.125

Standard errors in parentheses

\*  $p < 0.05$ , \*\*  $p < 0.01$ , \*\*\*  $p < 0.001$

*Notes:* Dependent variable: ancillary costs. First three columns correspond to the three clusters of load profiles for TenneT and last three columns for TransnetBW. Each regression includes two-way fixed effects of hour of the day, day of the week, month, and year. Only the coefficients relevant for the derivatives in the main text are reported. In all regressions we use only time observations for which the solar output is positive.

Table B.4: Effect of Solar Output on Ancillary Services Pooling All Observations

TSO	$\partial AS/\partial S$	
	quadratic	cubic
50Hertz	-0.46 (0.60)	-0.36 (0.66)
Amprion	-0.74 (0.59)	-0.64 (0.33)
TenneT	-0.31 (0.91)	-0.54 (0.46)
TransnetBW	-0.62 (0.38)	-0.44 (0.53)

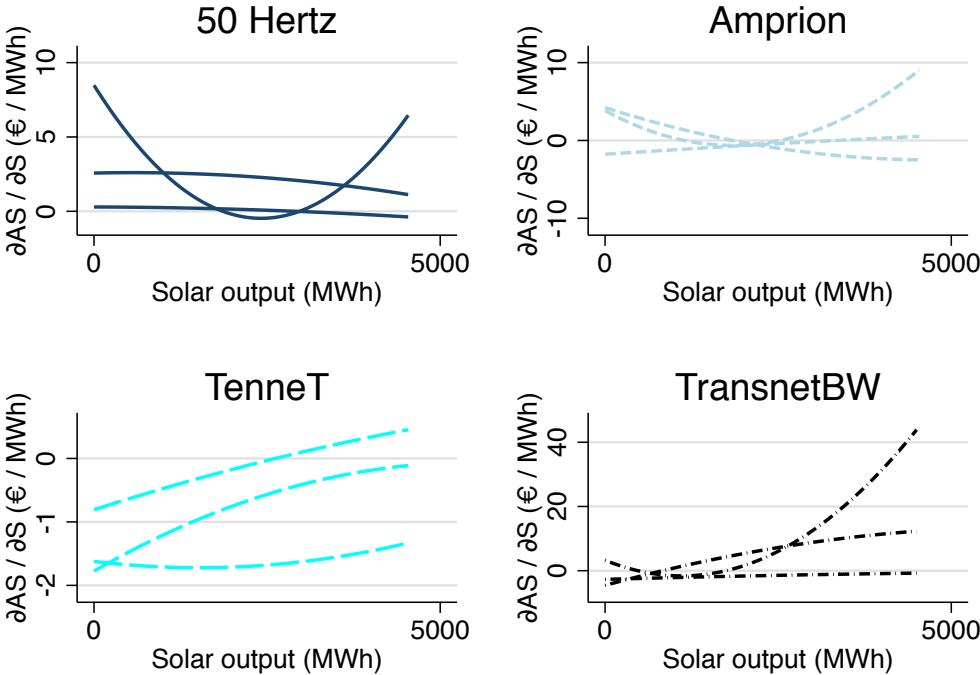
*Notes:* Each number, in €/ MWh, is the arithmetic mean of the values of  $\partial AS/\partial S$  when this derivative is evaluated at each 15-minute observation using the coefficients in [Table B.1](#). Standard deviations in parentheses.

Table B.5: Effect of Solar Output on Ancillary Services

TSO	$\partial AS/\partial S$		
	Low demand	Medium demand	High demand
50Hertz	2.23 (4.27)	0.17 (1.02)	0.16 (0.84)
Amprion	2.45 (4.28)	-0.75 (0.80)	1.92 (2.09)
TenneT	-0.09 (0.84)	-0.74 (0.70)	-0.31 (3.30)
TransnetBW	1.88 (4.90)	0.61 (4.03)	-1.06 (1.89)

*Notes:* Each number, in €/ MWh, is the arithmetic mean of the values of  $\partial AS/\partial S$  when this derivative is evaluated at each 15-minute observation using the coefficients in [Table B.2](#) and [Table B.3](#). Those coefficients were obtained using only observations for which  $S_{jt} > 0$ . The columns, labeled as “low”, “medium”, and “high”, correspond to each of the three clusters from [Figure B.1](#) from low to high demand levels. Standard deviations in parentheses.

Figure B.2: Effect of Solar Output on Ancillary Services Prices



*Notes:* Functions obtained using the coefficients from the main specification of the ancillary services costs regressions evaluated at the mean of load in the TSO and in each cluster of load. The three lines for each TSO correspond to each of the clusters of load profiles. The maximum value in the horizontal axis is the 90th percentile of the Germany-wide distribution of solar output, which is greater than the maximum solar output observed for TransnetBW.

## C Model of Transmission Capacity

This section closely follows [Joskow and Tirole \[2005\]](#) and [LaRiviere and Lyu \[2022\]](#). Assume region  $\mathcal{S}$  is a net exporter to region  $\mathcal{N}$  and it exports a quantity  $Q_{\mathcal{X},t}$  at time  $t$ , and that the marginal costs in each region ( $\lambda_{\mathcal{N},t}$  and  $\lambda_{\mathcal{S},t}$ ) are linear functions of the residual load  $S_{jt} - Q_{jt}$  and  $Q_{\mathcal{X},t}$ ,

$$\lambda_{\mathcal{N},t} = a_{\mathcal{N}} + b_{\mathcal{N}}(S_{\mathcal{N},t} - Q_{\mathcal{N},t}) + b_{\mathcal{N}}Q_{\mathcal{X},t}$$

and

$$\lambda_{\mathcal{S},t} = a_{\mathcal{S}} + b_{\mathcal{S}}(S_{\mathcal{S},t} - Q_{\mathcal{S},t}) + b_{\mathcal{S}}Q_{\mathcal{X},t}.$$

Also, we make the assumption that the coefficient on  $Q_{\mathcal{X},t}$  is the same as that of the residual load since the quantity traded does not change the slope of the supply or the demand for exports, it simply shifts the curves in a parallel manner to the left or to the right.

In the absence of transmission constraints,  $\lambda_{\mathcal{N},t} = \lambda_{\mathcal{S},t}$  because any arbitrage opportunity can be mitigated by buying or selling electricity from or to the other region. If there is a binding transmission constraint of size  $Q_{\mathcal{X},t} = K$  we can evaluate the two expressions above at that transmission level and write the marginal cost gap as

$$\lambda_{\mathcal{N},t} - \lambda_{\mathcal{S},t} = a_{\mathcal{N}} - a_{\mathcal{S}} + b_{\mathcal{N}}(S_{\mathcal{N},t} - Q_{\mathcal{N},t}) - b_{\mathcal{S}}(S_{\mathcal{S},t} - Q_{\mathcal{S},t}) + (b_{\mathcal{N}} - b_{\mathcal{S}})K.$$

Let  $z_t \equiv \lambda_{\mathcal{N},t} - \lambda_{\mathcal{S},t}$  and  $\Delta z_t \equiv z_t - z_{t-1}$ . Then, the change of the marginal cost gap with respect to the capacity of the transmission line is

$$\frac{\partial z_t}{\partial K} = b_{\mathcal{N}} - b_{\mathcal{S}}$$

and an interpretation of such derivative is that

$$\Delta K_t = \frac{\Delta z_t}{b_{\mathcal{N}} - b_{\mathcal{S}}},$$

from which we can infer the size of the capacity constraint given a change in the marginal cost difference between the two regions and the slopes of demand and supply of net exports. This process gives a distribution of the increments in the transmission capacity at each  $t$  for which  $z_t$  is above a pre-determined threshold.

Observe that  $\Delta K_t = 0$  if either  $z_t = z_{t-1} > 0$  or if  $z_t = z_{t-1} = 0$ . Therefore, by using the expression for  $\Delta K_t$  it is not possible to distinguish whether a value of 0 for the transmission capacity is due to observing the same marginal cost gap in two consecutive periods or because the price gap was indeed zero in two consecutive periods. This calls for using an aggregation of the different values of  $\Delta K_t$ , let  $\overline{\Delta K}$  be the mean of that distribution. Then, the imputed marginal cost in region  $\mathcal{N}$  can be written as

$$\lambda_{\mathcal{N},t} = \lambda_{\mathcal{S},t} + z_{t-1} + (b_{\mathcal{N}} - b_{\mathcal{S}})\overline{\Delta K}.$$

To estimate the parameters  $b_{\mathcal{N}}$  and  $b_{\mathcal{S}}$  we need exogenous variation and fixed-effects that solve the natural endogeneity problem between the residual demand ( $S_{jt} - Q_{jt}$ ) and the

marginal costs ( $\lambda_{jt}$ ). To that end we use the load in region  $k$  to estimate the slope in region  $j \neq k$  since once the transmission constraint is being used at full capacity, any additional load in  $k$  has no effect on the production costs in region  $j$ . Note that since we do not observe the quantities traded, we omit the terms  $b_N Q_{X,t}$  and  $b_S Q_{X,t}$  from the estimation equations. This discussion motivates the following equations that we estimate in the main text,

$$\begin{aligned} E[\lambda_{N,t}] &= a_N + b_N(S_{N,t} - Q_{N,t}) + c_N Q_{S,t} + FE_s \\ E[\lambda_{S,t}] &= a_S + b_S(S_{S,t} - Q_{S,t}) + c_S Q_{N,t} + FE_s. \end{aligned}$$

## D Additional Tables and Figures

Table D.1: Simulated Frequencies of Marginal Technologies (by TSO)

TSO: 50Hertz			TSO: Amprion		
Source	Freq.	Percent	Source	Freq.	Percent
Natural Gas	69,954	99.68	Natural Gas	68,868	98.14
Hard Coal	152	0.22	Hard Coal	1,308	1.86
Hydro: River	46	0.07			
Hydro: Pumped storage	24	0.03			

TSO: TenneT			TSO: TransnetBW		
Source	Freq.	Percent	Source	Freq.	Percent
Hard Coal	41,330	58.89	Hard Coal	57,975	82.61
Natural Gas	27,157	38.70	Natural gas	6,522	9.29
Oil	1,030	1.47	Nuclear	3,522	5.02
Brown Coal / Lignite	655	0.93	Oil	2,157	3.07
Biomass	4	0.01			

*Notes:* For each 15-minute interval we compute the marginal cost of each of the technologies shown in the tables and sort them from lowest to highest marginal cost to obtain the system’s marginal cost curve. Notice that the marginal cost for fossil fuels can change over time as we use fuel prices to construct this curve. Finally, we select the technology that corresponds to the point in the marginal cost curve that intersects the net load in that time interval. TenneT and TransnetBW display large frequencies for hard coal being the marginal technology. This has been observed also by market analysts (see [Timera Energy \[2014\]](#)).

Table D.2: Ranking of TSOs by Output per Unit of Capacity Installed

	(1)	(2)	(3)
TransnetBW	907.331*** (31.821)	988.127*** (35.940)	1037.727*** (38.489)
Amprion	818.864*** (22.174)	927.586*** (30.437)	971.994*** (32.935)
50 Hertz	820.226*** (33.770)	912.942*** (37.201)	966.330*** (41.332)
TenneT	806.680*** (22.579)	894.915*** (28.738)	965.630*** (33.769)
Controls:			
Year	✓	✓	✓
Panel orientation		✓	✓
Panel shading		✓	✓
Inverter size		✓	✓
Panel tilt			✓
$N$	485	485	464
$R^2$	0.920	0.928	0.930

Standard errors in parentheses

\*  $p < 0.05$ , \*\*  $p < 0.01$ , \*\*\*  $p < 0.001$

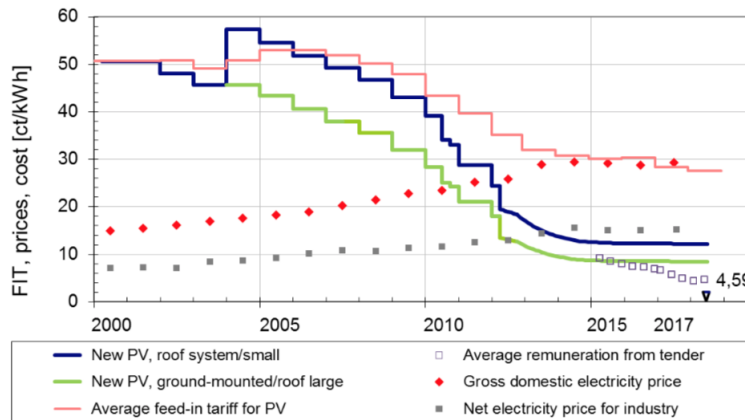
*Notes:* Dependent variable: output in kWh per kW of capacity installed. Control variables are included as categorical variables. The reference (omitted) category in column 2 are South facing solar plants with no shading and a large inverter size ( $> 7$  kW). Column 3 additionally conditions on tilt (15-40 degrees as omitted category). For each column, the magnitude of the coefficients define the ranking in solar productivity.

Table D.3: Estimates of Shadow Costs of Transmission (additional specifications)

	(1)	(2)	(3)	(4)	(5)	(6)
	Gap > 2 €/ MWh		Gap > 5 €/ MWh		Gap > 8 €/ MWh	
	$\lambda_N$	$\lambda_S$	$\lambda_N$	$\lambda_S$	$\lambda_N$	$\lambda_S$
$S_N - Q_N$	-0.00135*** (0.000326)		-0.00140*** (0.000327)		-0.000922* (0.000431)	
$Q_S$	-0.00437*** (0.00109)		-0.00444*** (0.00109)		-0.00485*** (0.00132)	
$S_S - Q_S$		-0.00636*** (0.000583)		-0.00654*** (0.000603)		-0.00722*** (0.000673)
$Q_N$		0.00205 (0.00109)		0.00226* (0.00111)		0.00381** (0.00136)
<i>Load in other TSOs:</i>						
50Hertz	0.000471* (0.000209)	-0.0000675 (0.000422)	0.000447* (0.000209)	-0.0000306 (0.000423)	0.000381 (0.000210)	0.000204 (0.000504)
Amprion	0.000480 (0.000268)	0.000612 (0.000603)	0.000553* (0.000266)	0.000622 (0.000604)	0.000876** (0.000291)	0.000318 (0.000703)
TransnetBW	0.00176** (0.000617)	-0.000965 (0.00136)	0.00159** (0.000613)	-0.00104 (0.00138)	0.00133 (0.000689)	-0.00155 (0.00154)
Constant	5.972 (5.047)	-29.29** (10.52)	5.728 (5.093)	-32.46** (10.48)	8.645 (5.700)	-45.04*** (12.42)
$N$	4,377	4,377	4,315	4,315	3,719	3,719
$R^2$	0.825	0.712	0.828	0.715	0.838	0.710

*Notes:* Dependent variable: as indicated on top of each column. “Gap” is the absolute value of the difference between the two marginal costs. Regression includes additional controls for load in other TSOs. Standard errors clustered at the date level. \*  $p < 0.05$ , \*\*  $p < 0.01$ , \*\*\*  $p < 0.001$ .

Figure D.1: Evolution of FiTs for Solar (Germany)

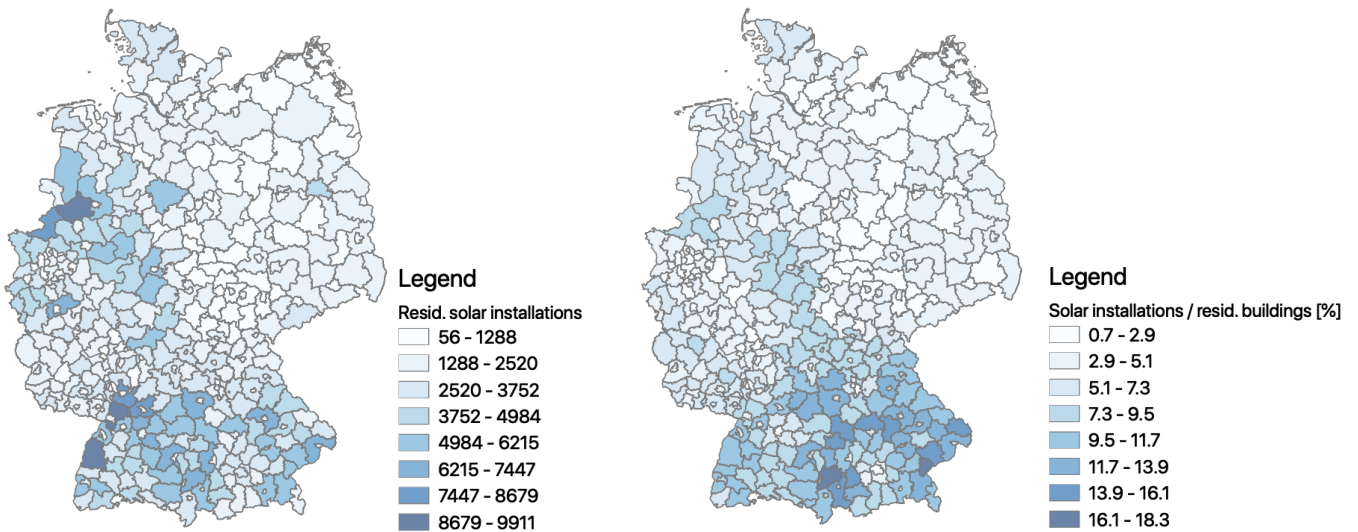


Notes: Taken from Fraunhofer ISE Philipps and Warmuth [2018].

Figure D.2: Residential Solar Installations

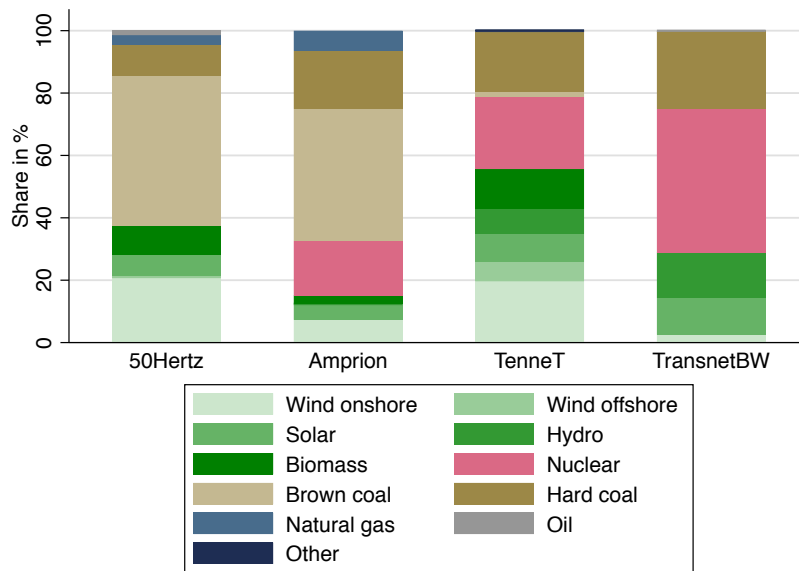
a: Cumul. Solar Uptake

b: Cumul. Solar Uptake / Resid. Bldgs.



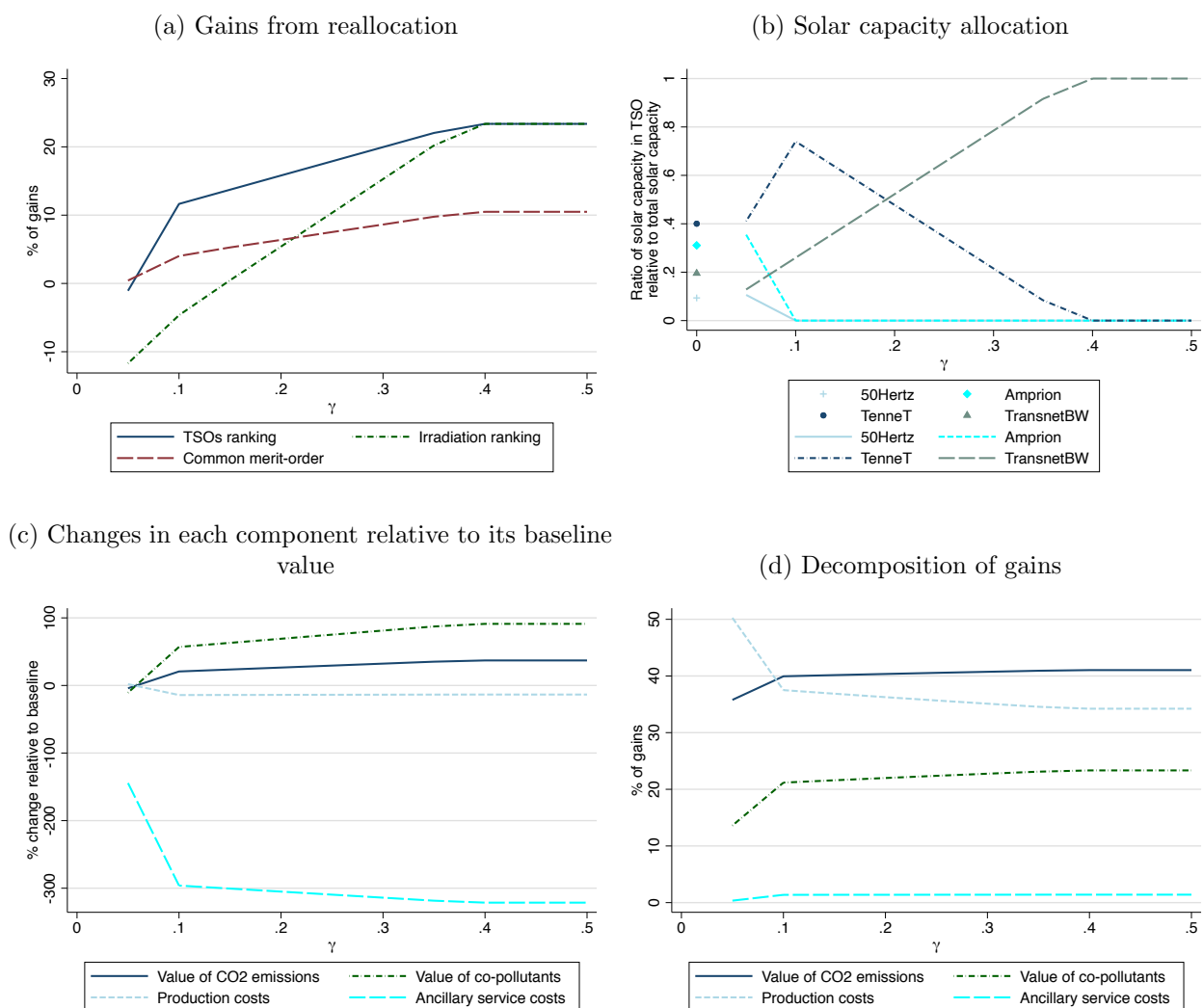
Notes: Cumulative residential solar installations (Dec 2016), with a maximum installed capacity of 10 kW (Panel a). Cumulative solar installations over residential buildings in Panel b. Darker areas represent more solar capacity installed and higher penetration rates, respectively.

Figure D.3: Technology Portfolio Mix by TSO, Production 2015-16



Notes: Average technology shares in electricity production 2015-16. Source: [ENTSO-E \[2018\]](#).

Figure D.4: Value of reallocation when including co-pollutants



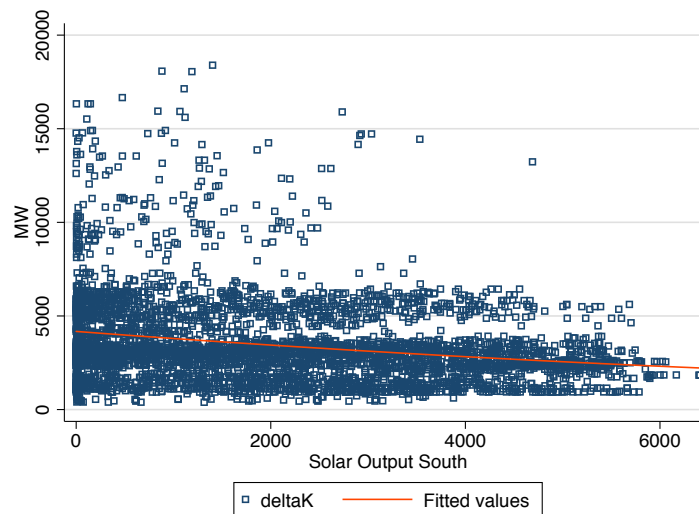
Notes: Gains from reallocation and solar capacity shares when including co-pollutants, as highlighted in Table 1. Social cost of carbon (SCC) equal to 31.71 €/tCO<sub>2</sub> assumed.

Figure D.5: Planned Extension of High Voltage Network



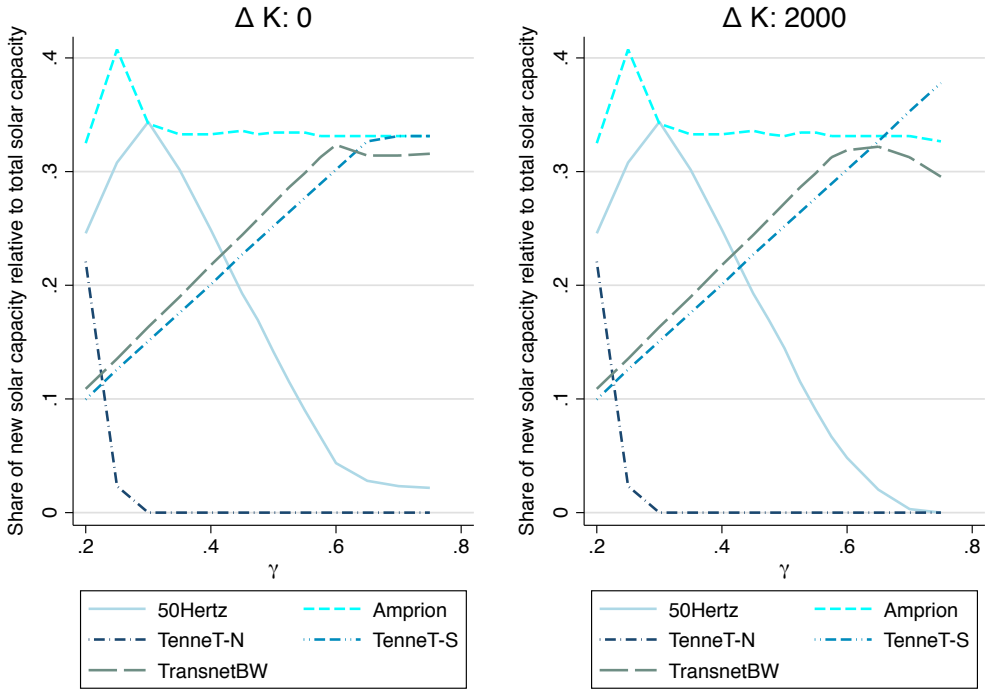
Notes: Network Development Plan [2019].

Figure D.6: Implied Transmission Capacities



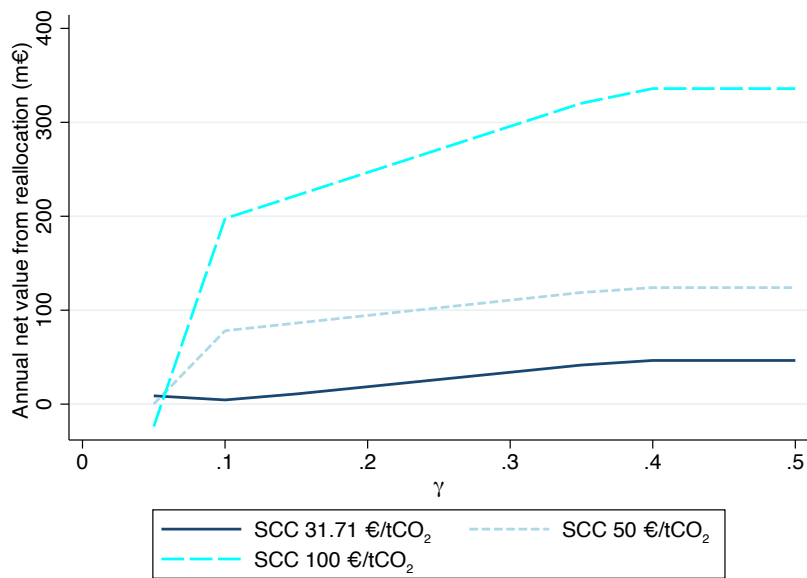
Notes: Each square represents one of the values obtained using Equation (2). The overall mean is 3,487 MW.

Figure D.7: 5 TSO with Transmission: Solar capacity allocation by TSO



Notes: Solar capacity allocation as function of  $\gamma$  with and without interconnection between TenneT South (export region) and TenneT North.

Figure D.8: Reallocation gains net of subsidy expenses



*Notes:* We define the policy's net gains as

(value in reallocation – value in baseline) – (subsidy in reallocation – subsidy in baseline).

## References

- Bahn, O., Samano, M., and Sarkis, P. (2020). Market Power and Renewables: The Effects of Ownership Transfers. *Energy Journal*.
- Consentec GmbH (2016). Konventionelle Mindestenerzeugung – Einordnung, aktueller Stand und perspektivische Behandlung. <https://www.consentec.de/publikationen/studien>. Last accessed July 31, 2021.
- EIA (2020). Capacity Factors for Utility Scale Generators Primarily Using Non-Fossil Fuels. [https://www.eia.gov/electricity/monthly/epm\\_table\\_grapher.php?t=epmt\\_6\\_07\\_b](https://www.eia.gov/electricity/monthly/epm_table_grapher.php?t=epmt_6_07_b). Last accessed September 23, 2021.
- Energy Brain Pool (2017). What is the Minimum CO<sub>2</sub>-price in Order to Affect the Merit-order? <https://blog.energybrainpool.com/en/what-is-the-minimum-co2-price-in-order-to-affect-the-merit-order>. Last accessed September 19, 2021.
- ENTSO-E (2018). TYNDP (Network Development Plan). <https://tyndp.entsoe.eu/tyndp2018>. Last accessed June 9, 2020.
- German Environmental Ministry (2017). Daten und Fakten zu Braun- und Steinkohlen. [https://www.umweltbundesamt.de/sites/default/files/medien/1410/publikationen/171207\\_uba\\_hg\\_braunsteinkohle\\_bf.pdf](https://www.umweltbundesamt.de/sites/default/files/medien/1410/publikationen/171207_uba_hg_braunsteinkohle_bf.pdf). Last accessed September 23, 2021.
- Germeshausen, R. and Wölfling, N. (2020). How Marginal is Lignite? Two Simple Approaches to Determine Price-setting Technologies in Power Markets. *Energy Policy*, 142:111482.
- Green, R., Staffell, I., and Vasilakos, N. (2011). Divide and Conquer? Assessing k-means Clustering of Demand Data in Simulations of the British Electricity System. Technical report, Available from <http://tinyurl.com/c934prp>.
- Holland, M., Pye, S., Watkiss, P., Droste-Franke, B., and Bickel, P. (2005). Damages per Tonne Emission of PM<sub>2.5</sub>, NH<sub>3</sub>, SO<sub>2</sub>, NO<sub>x</sub> and VOCs from each EU25 Member State (excluding Cyprus) and Surrounding Seas. Last accessed July 7, 2021.
- Joskow, P. and Tirole, J. (2005). Merchant Transmission Investment. *The Journal of Industrial Economics*, 53(2):233–264.
- LaRiviere, J. and Lyu, X. (2022). Transmission Constraints, Intermittent Renewables and Welfare. *Journal of Environmental Economics and Management*.
- Neon Neue Energieökonomik, Technical University of Berlin, DIW Berlin, and ETH Zürich (2019). Open Power System Data. <https://open-power-system-data.org>. Last accessed February 7, 2022.
- Network Development Plan (2019). Network Development Plan 2030. <https://www.netzentwicklungsplan.de/de/projekte/projekte-nep-2030-2019>. Last accessed February 7, 2022.

- Philipps, S. and Warmuth, W. (2018). Photovoltaics Report. <https://www.ise.fraunhofer.de/en/publications/studies/photovoltaics-report.html>. Fraunhofer ISE and PSE Projects GmbH. Last accessed September 23, 2021.
- PV Output (2020). PV Output Data. <https://pvoutput.org>. Last accessed June 9, 2020.
- Reguant, M. (2019). The Efficiency and Sectoral Distributional Impacts of Large-scale Renewable Energy Policies. *Journal of the Association of Environmental and Resource Economists*, 6(S1):S129–S168.
- Staudt, P., Rausch, B., and Weinhardt, C. (2019). Congestion data TSO 50 Hertz Germany 2015-2017. <https://publikationen.bibliothek.kit.edu/1000089656>. Karlsruher Institute for Technology. Last accessed September 23, 2021.
- Timera Energy (2014). German Recession, Power Prices & Generation Margins. <https://timera-energy.com/german-recession-power-prices-generation-margins>. Last accessed June 12, 2019.